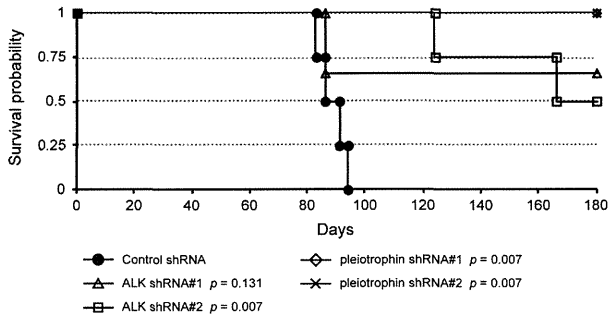

Figure 3. ALK and pleiotrophin are critical for the tumorigenicity of GSCs. GB2 cells maintained in serum-free medium were infected with a lentivirus expressing an shRNA-targeting ALK or pleiotrophin. One week after infection, cells were transplanted into the frontal lobe of immunodeficient mice. *P*-values with comparison to control shRNA by log rank test are shown.

mutation in the *ALK* gene in GB2 cells, consistent with the results of a comprehensive genome analysis reported previously.[29,30] It is known that pleiotrophin is highly expressed in GSCs (Figure 1). We therefore examined the transcriptional control of *pleiotrophin* in GSCs. We found that pleiotrophin protein and mRNA expression levels decreased during serum-induced differentiation, similar to what was observed for the stem cell markers (Figure 4a). Moreover, retinoic acid-induced differentiation also resulted in a decrease in the levels of pleiotrophin[31] (Figure 4b). We also investigated the expression profiles of *pleiotrophin* obtained from a public microarray database.[3] Almost all patient glioblastomas and two GSC lines as well as NSCs expressed substantial levels of *pleiotrophin* (Figure 4c). By contrast, glioma cell lines and two GSC lines cultured in serum-containing medium expressed relatively low levels of *pleiotrophin*, presumably because they had undergone 'differentiation'.[3] These results suggest that high expression of pleiotrophin is a common feature of GSCs.

SOX2 directly transactivates the expression of pleiotrophin in GSCs

To further investigate the mechanisms underlying the expression of *pleiotrophin*, we performed reporter assays using a *luciferase* reporter under the control of the full-length *pleiotrophin* 5′ region (-1401 to $+309$) and several deletion variants. When transfected into GB2 cells, a reporter containing the region between -251 and $+309$ showed a substantial level of activity (Figure 5a, left panel). Furthermore, this activity was repressed upon serum-induced differentiation. We therefore attempted to identify the transcription factor(s) involved in modulating this promoter activity. We first searched the region -251 and $+309$ for transcription factor consensus binding sites and then compared the expression patterns of the selected transcription factors and pleiotrophin using a microarray database.[3] We found that the expression pattern of *pleiotrophin* is similar to that of *SOX2* (Figure 4c). Furthermore, a mutant reporter lacking the SOX2-binding site (-40 to -21) showed reduced promoter activity (Figure 5a, right panel). Chromatin immunoprecipitation analysis demonstrated that endogenous SOX2 was present at the *pleiotrophin* promoter in GSCs (Figure 5b and Supplementary Figure S3A). Consistent with these results, silencing of SOX2 by shRNA resulted in a decrease in the levels of pleiotrophin protein and mRNA (Figure 5c and Supplementary Figure S3B). Similar results were obtained by transfecting two different siRNAs targeting SOX2 (Supplementary Figure S3C). These results suggest that SOX2 stimulates transcription of the *pleiotrophin* gene, thereby maintaining high expression levels of pleiotrophin in GSCs.

DISCUSSION

It has been reported that ALK acquires oncogenic potential when truncated and fused to a partner protein, such as NPM, as can occur via chromosomal rearrangement.[7,8] It has also been reported that ALK is activated by point mutations in its kinase domain in some neuroblastoma.[7,32] Although we could not identify any chromosomal rearrangement or point mutation in ALK in GB2 cells, we found that ALK is highly expressed in GSC lines cultured in serum-free medium, consistent with previous reports.[33] Furthermore, we showed that knockdown of ALK results in a decrease in the self-renewing capacity and tumorigenicity of GB2 cells. We also found that pleiotrophin is overexpressed both in patient glioblastomas and in GSC lines cultured in serum-free medium and that knockdown of pleiotrophin leads to a reduction in the self-renewing capacity and tumorigenicity of GB2 cells. Thus, our results suggest that the pleiotrophin-ALK axis is required for the self-renewal and tumorigenicity of GSCs.

NPM-ALK, the most thoroughly studied ALK-fusion protein, has been reported to signal via the MAP kinase, phospholipase Cγ, PI3-kinase and JAK/STAT pathways.[7] Consistent with these reports, our DNA array analysis revealed that the MAP kinase, PI3-kinase and JAK/STAT pathways are activated in GSCs. Furthermore, we found that ALK and pleiotrophin activate the Myc and ESC-like transcriptional programs, which are known to be associated with more aggressive phenotypes in human cancers.[25,27] Activation of these pathways by ALK has not been previously reported, presumably because earlier studies utilized cultured cell lines grown in serum-containing media that do not exhibit any stem cell-like properties. We found that there was only about a 30% overlap between the genes dependent on ALK and pleiotrophin expression. Furthermore, only pleiotrophin, but not ALK, activated the Wnt signaling pathway. These results appear to be in line with the fact that pleiotrophin signals not only via ALK but also via other receptors, such as RPTPβ/ζ (receptor protein tyrosine phosphatase β/ζ) and N-syndecan.[34,35] Interestingly, pleiotrophin is known to stimulate tyrosine phosphorylation of β-catenin through inactivation of RPTPβ/ζ.[34] Furthermore, pleiotrophin stimulates tumor angiogenesis and remodeling of the microenvironment.[36] Consistent with these findings, we found that repression of pleiotrophin has a more dramatic effect on the tumorigenicity of GSCs than repression of ALK.

It has been reported that SOX2 is involved in the tumorigenesis of several cancers, including lung cancer and breast cancer.[37–39] We found that SOX2 directly transactivates the expression of pleiotrophin in GSCs. Our results appear to be consistent with a previous report showing that knockdown of SOX2 suppresses the tumorigenicity of GSCs in immunodeficient mice.[17] Thus, SOX2-mediated transactivation of pleiotrophin may be important for the tumorigenicity of GSCs. However, knockdown of SOX2 only partially reduced the expression levels of pleiotrophin (Figure 5c and Supplementary Figures 3B and C), and mutation of the SOX2-binding site in the pleiotrophin promoter only partially reduced activity of a luciferase reporter (Figure 5a, right panel). In addition, we found that the levels of pleiotrophin decreased faster than those of SOX2 during serum-induced differentiation (Figure 4a) and that retinoic acid-induced differentiation resulted in a drastic decrease in the expression levels of pleiotrophin but not of SOX2 (Figure 4b). Thus, the pleiotrophin-ALK axis may be regulated by other transcription factors in addition to SOX2.

SOX2 is well known to have critical roles in the maintenance of neural stem and progenitor cells.[14,15] For example, it has been reported that multipotent neural stem-like cells transfected with an siRNA targeting SOX2 express increased neurofilaments but decreased GFAP and Nestin levels.[40] These results suggest that SOX2 inhibits the differentiation of neural stem-like cells into neurons and maintains their stem-like properties. Intriguingly, our results appear to be consistent with these results. We found that

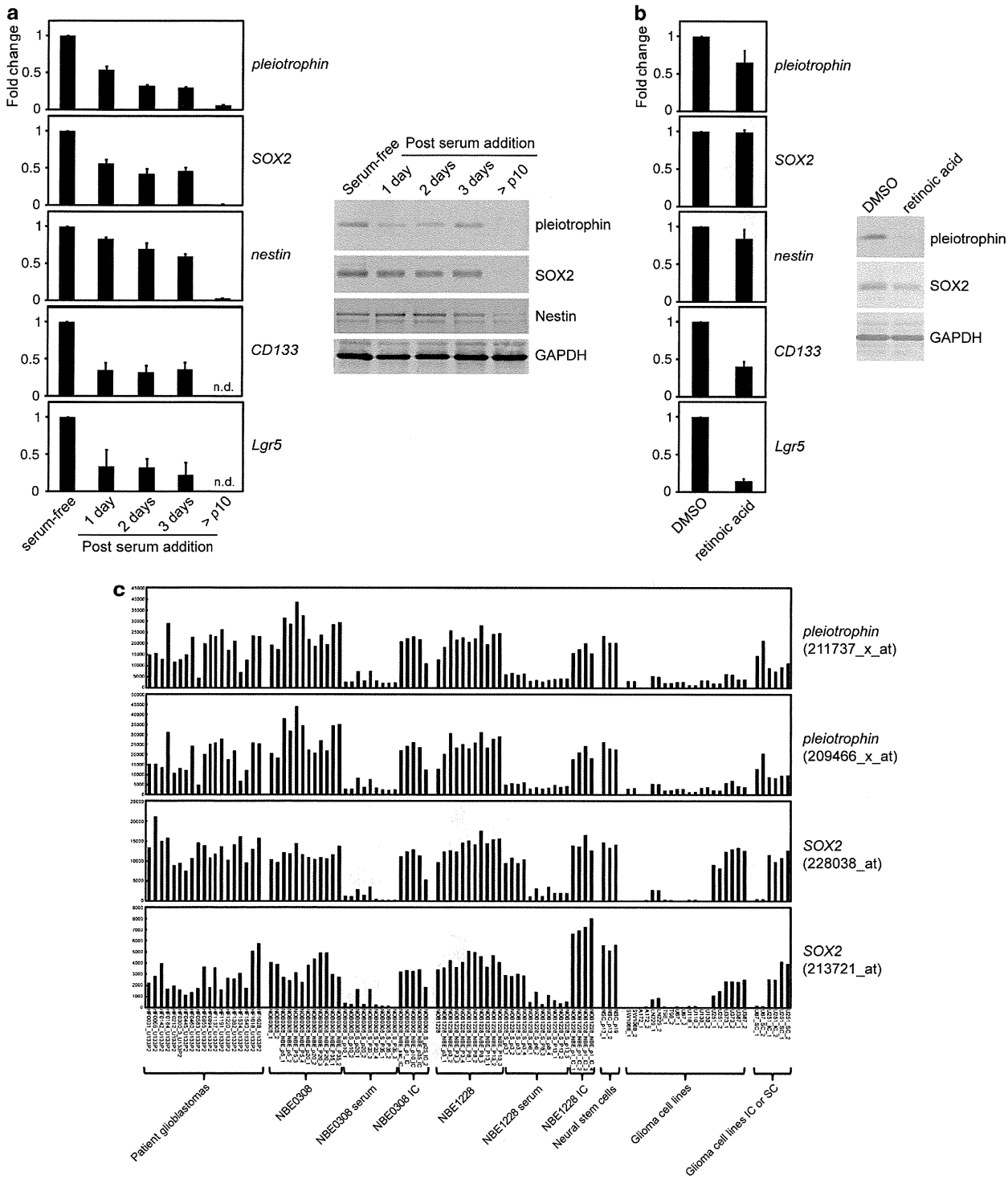

Figure 4. High expression of pleiotrophin in GSCs. (**a**) GB2 cells maintained in serum-free medium were cultured in serum-containing medium for the indicated times. >p10, GB2 cells cultured in serum-containing medium for >10 passages. The mRNA levels of the indicated genes were evaluated by quantitative RT–PCR and shown as the fold change over mRNA levels in GB2 cells maintained in serum-free medium (left). Error bars represent the s.d. ($n = 3$). ND, not detected. Cell lysates were subjected to immunoblotting with antibodies to the indicated proteins (right). CD133 and Lgr5 could not be detected by immunoblotting because of their low expression levels. (**b**) GB2 cells maintained in serum-free medium were cultured in medium containing retinoic acid for 4 days. The mRNA levels of the indicated genes were evaluated by quantitative RT–PCR and shown as the fold change over the vehicle-treated cells (left). Error bars represent the s.d. ($n = 3$). Cell lysates were subjected to immunoblotting with antibodies to the indicated proteins (right). (**c**) Gene expression profiles of *pleiotrophin* and *SOX2* taken from the public microarray database GSE4536 (Lee *et al.*[3]). Data obtained with two independent probes for each gene are shown. NBE0308 and NBE1228 are GSC lines. Serum, GSCs cultured in serum-containing medium; IC, intracranial injection; SC, subcutaneous injection.

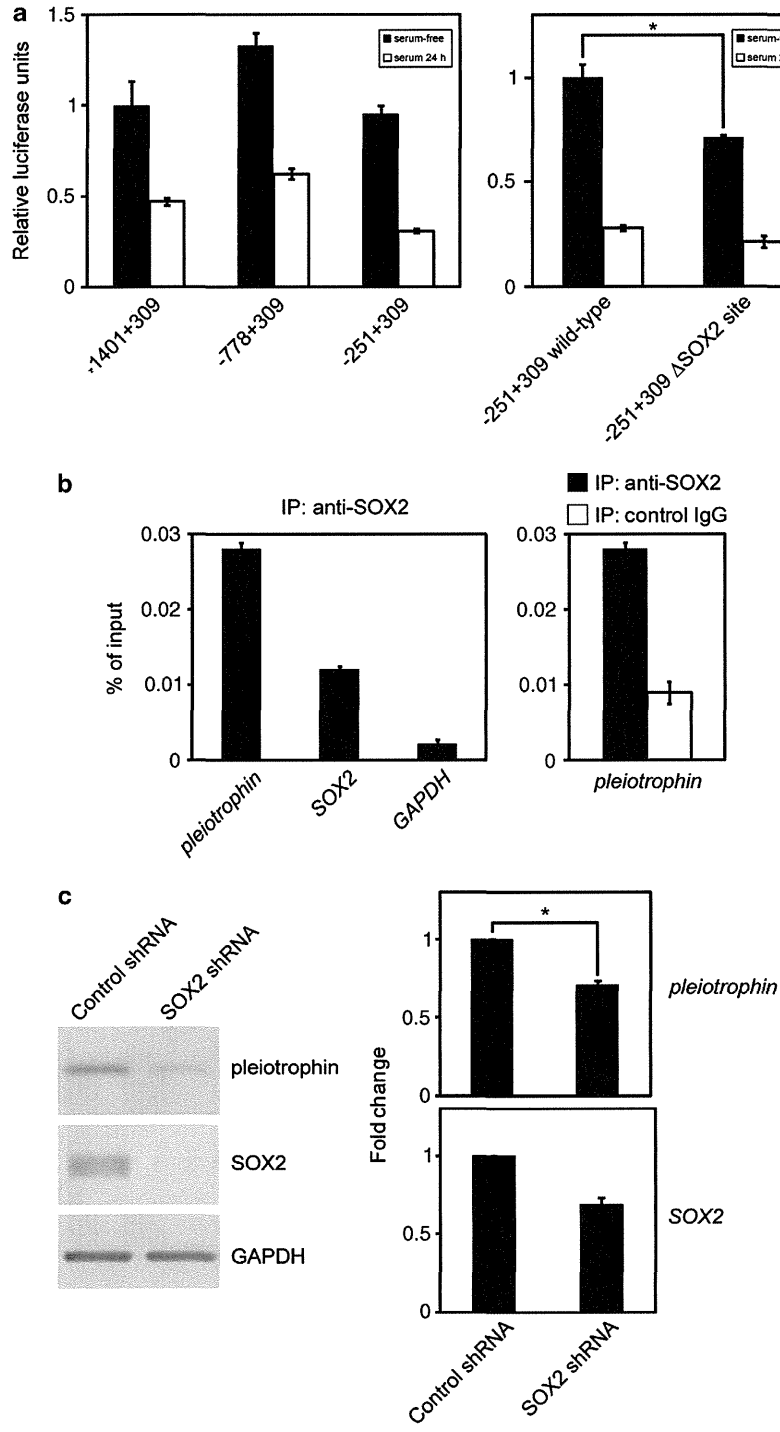

Figure 5. SOX2 directly transactivates the expression of pleiotrophin in GSCs. (**a**) GB2 cells maintained in serum-free medium were transfected with a luciferase reporter driven by the *pleiotrophin* promoter. Luciferase reporter activity is shown. Error bars represent the s.d. ($n = 3$). *$P = 0.0058$ by *t*-test. (**b**) Chromatin immunoprecipitation experiments with anti-SOX2 antibody were performed with GB2 cells maintained in serum-free medium. The precipitated chromatin was amplified by quantitative PCR using primers flanking the indicated gene promoters (*pleiotrophin* and *GAPDH*) or enhancer (*SOX2*) (left). The *SOX2* enhancer was used as a positive control, as SOX2 has been reported to be autoregulated.[50] The *GAPDH* promoter was used as a negative control. Control IgG was used as a negative control (right). Error bars represent the s.d. ($n = 3$). (**c**) GB2 cells maintained in serum-free medium were infected with a lentivirus expressing an shRNA-targeting SOX2. Cell lysates were subjected to immunoblotting with antibodies to the indicated proteins (left). The mRNA levels of the indicated genes were evaluated by quantitative RT–PCR and shown as the fold change over mRNA levels in cells expressing control shRNA (right). Error bars represent the s.d. ($n = 3$). *$P = 0.001$ by *t*-test.

GSCs infected with a lentivirus expressing an shRNA targeting ALK or pleiotrophin have increased MAP2 but decreased GFAP, Olig2 and Nestin levels. These results suggest that the pleiotrophin-ALK axis inhibits neural differentiation of GSCs but maintains their stem-like characteristics. It would be interesting to examine whether the pleiotrophin-ALK axis is also involved in the maintenance of normal neural stem and progenitor cells. SOX2 has also been reported to have essential roles in the neuronal differentiation of subsets of neural stem and progenitor cells.[14,15] For example, it has been reported that SOX2 deficiency causes impaired neurogenesis and neurodegeneration in the adult mouse brain.[41,42] Therefore, it would be interesting to investigate whether the pleiotrophin-ALK axis is also involved in the differentiation of neural stem and progenitor cells.

The ALK inhibitor crizotinib has recently been approved for the treatment of metastatic and late stage ALK-positive NSCLC having translocations of the ALK gene.[9,10] In addition, the ALK inhibitor TAE684 has been reported to inhibit the growth of ALK-positive ALCL, neuroblastoma and NSCLC cell lines.[43] Thus, we speculate that ALK inhibitors may be effective for the treatment of glioblastoma. ALK has been assumed to have a role in the development and function of the central and peripheral nervous system, as ALK is abundantly expressed in the nervous system during mouse embryogenesis,[7] which could raise concerns about the safety of such therapy. However, both ALK- and pleiotrophin-mutant mice survive as long as wild-type mice.[7,44] In addition, although pleiotrophin is highly expressed in NSCs, it seems dispensable for their proliferation *in vivo*.[45] Furthermore, it has been reported that the most common adverse reactions of crizotinib are relatively minor, consisting of vision disorder, nausea, diarrhea, vomiting, edema and constipation.[46] Thus, compounds targeting ALK or pleiotrophin would be expected to have relatively few serious side effects due to their effects on NSCs. In addition, we imagine that antibodies or compounds that specifically target the extracellular domain of ALK or pleiotrophin could also hold promise as novel anti-tumor reagents.

MATERIALS AND METHODS

Tumor specimens and primary tumor cultures

Tumor samples classified as primary glioblastoma were obtained from patients undergoing surgical treatment at the University of Tokyo Hospital with informed consent and as approved by the Institutional Review Board. Tumors were washed and mechanically and enzymatically dissociated into single cells. Tumor cells were cultured in Neurobasal medium (Life Technologies, Carlsbad, CA, USA) containing B27 supplement minus vitamin A (Life Technologies), EGF and FGF2 (20 ng/ml each; Wako Pure Chemical Industries, Osaka, Japan). For *in vitro* differentiation, tumor cells were cultured in DMEM (Dulbecco's modified Eagle's medium)/F-12 medium (Life Technologies) containing 10% fetal bovine serum or 10 μM all-trans retinoic acid (Sigma, St. Louis, MO, USA). U87 and 293FT cells were cultured in DMEM (Nissui, Tokyo, Japan) containing 10% fetal bovine serum. Transfections were performed using Lipofectamine 2000 Reagent, Lipofectamine LTX Reagent or Lipofectamine RNAiMAX Reagent (Life Technologies).

RNAi

Silencer Select Human Extended Druggable Genome siRNA Library was purchased from Life Technologies (the list is given in Supplementary Table S1). The siRNA oligonucleotide sequences were as follows: SOX2#1 (5′-CAGUAUUUAUCGAGAUAAA-3′), and SOX2#2 (5′-AGUG GAAACUUUUGUCGGA-3′).

The shRNA oligonucleotide sequences were as follows: ALK#1 (5′-GGCCU GUAUACCGGAUAAUGA-3′), ALK#2 (5′-GAAUACAGCACCCAAAUCAAG-3′), pleiotrophin#1 (5′-GGAGCUGAGUGCAAGCAAACC-3′), pleiotrophin#2 (5′-GCAACUGGAAGAAGCAAUUUG-3′), and SOX2 (5′-GUAAGAAACAGCAUG GAGAAA-3′).

Quantitative RT–PCR

Total RNA was extracted using the NucleoSpin RNA Clean-up kit (Takara Bio Inc., Shiga, Japan) and reverse-transcribed into cDNA using PrimeScript RT Master Mix (Takara Bio Inc.). Real-time PCR was performed using LightCycler480 SYBR Green I Master and a LightCycler480 Instrument (Roche, Indianapolis, IN, USA). The results were normalized with the detected value for glyceraldehyde-3-phosphate dehydrogenase (*GAPDH*) or hypoxanthine phosphoribosyltransferase 1 (*HPRT1*). Primers used in real-time PCR were as follows: *GAPDH* forward (5′-GCACCGTCAAGGCTGA GAAC-3′), *GAPDH* reverse (5′-TGGTGAAGACGCCAGTGGA-3′); *HPRT1* forward (5′-GGCAGTATAATCCAAAGATGGTCAA-3′), *HPRT1* reverse (5′-GTCA AGGGCATATCCTACAACAAAC-3′); *CD133* forward (5′-AGTGGCATCGTGCA AACCTG-3′), *CD133* reverse (5′-CTCCGAATCCATTCGACGATAGTA-3′); *nestin* forward (5′-GAGGTGGCCACGTACAGG-3′), *nestin* reverse (5′-AAGCTGAGGG AAGTCTTGGA-3′); *Lgr5* forward (5′-GATTTCCTGCTTGACTTTGAGG-3′), *Lgr5* reverse (5′-GCAGGTGTTCACAGGGTTTG-3′); *SOX2* forward (5′-TTGCTGCCTC TTTAAGACTAGGA-3′), *SOX2* reverse (5′-CTGGGGCTCAAACTTCTCTC-3′); *ALK* forward (5′-CACTCCAGGGAAGCATGG-3′), *ALK* reverse (5′-TCGAAATGGGTT GTCTGGA-3′); *pleiotrophin* forward (5′-AACTGACCAAGCCCAAACCT-3′), *pleiotrophin* reverse (5′-GGTGACATCTTTTAATCCAGCA-3′), *MAP2* forward (5′-TCTCCTGTGTTAAGCGGAAAA-3′), *MAP2* reverse (5′-AATACACTGGGAGC CAGAGC-3′), *GFAP* forward (5′-GACCTGGCCACTGTGAGG-3′), *GFAP* reverse (5′-AGGCAGCCAGGTTGTTCTC-3′), *Olig2* forward (5′-AGCTCCTCAAATCGC ATCC-3′), and *Olig2* reverse (5′-ATAGTCGTCGCAGCTTTCG-3′).

Antibodies

Rabbit polyclonal antibody (pAb) to green fluorescence protein (GFP) and goat pAb to SOX2 were obtained from Santa Cruz Biotechnology (Santa Cruz, CA, USA). Rabbit pAbs to ALK were from Cell Signaling Technology (Danvers, MA, USA). Mouse monoclonal antibody (mAb) to pleiotrophin (H-6) was from Santa Cruz Biotechnology. Mouse mAb to Nestin was from R&D systems (Minneapolis, MN, USA). Mouse mAb to GAPDH was from Millipore (Bedford, MA, USA).

Immunoblotting

Cells were lysed in lysis buffer (50 mM Tris-HCl (pH 7.5), 150 mM NaCl, 1% Triton X-100, 1 mM DTT, 1 mM EDTA, 2 mM Na_3VO_4, 10 mM NaF and protease inhibitors. Lysates were fractionated by SDS–PAGE (sodium dodecyl sulfate-polyacrylamide gel electrophoresis) and transferred to a PVDF (polyvinylidene difluoride) membrane (Immobilon-P, Millipore). The membrane was subjected to immunoblot analysis using alkaline phosphatase-conjugated anti-mouse immunoglobulin G (IgG) or anti-rabbit IgG (Promega, Madison, WI, USA) as secondary antibodies. Visualization was performed using the NBT/BCIP colorimetric substrate system (Promega).

Lentivirus production

A lentiviral vector (CS-Rfa-CG) expressing an shRNA driven by the H1 promoter was transfected together with the packaging vectors pCAG-HIV-gp and pCMV-VSV-G-RSV-Rev into 293FT cells. All plasmids were kindly provided by H. Miyoshi (RIKEN BioResource Center, Ibaraki, Japan). Virus supernatant was purified by ultracentrifugation at 25 000 r.p.m. for 90 min (SW28 rotor, Beckman Coulter, Brea, CA, USA). Infection efficiency was monitored by GFP expression driven by the CMV promoter.

Intracranial xenograft

One week after lentivirus infection, 1×10^4 cells were injected stereotactically into the right frontal lobe of 5-week-old nude mice (BALB/cAJcl-*nu/nu*, CLEA Japn Inc., Tokyo, Japan), following administration of general anesthesia ($n = 3$ or 4). The injection coordinates were 2 mm to the right of the midline, 1 mm anterior to the coronal suture and 3 mm deep. Mice were monitored for 6 months. Survival of mice was evaluated by Kaplan–Meier analysis. *P*-values were calculated using log rank test. The distribution of tumor cells was analyzed by GFP immunostaining. Tumors were histologically analyzed after hematoxylin and eosin staining. All animal experimental protocols were performed in accordance with the guidelines of the Animal Ethics Committee of the University of Tokyo.

Immunohistochemistry

Three months after injection of cells, brains were fixed in 3.7% buffered formalin, dehydrated and embedded in paraffin. Sections (6 μm) were rehydrated, and endogenous peroxidases were blocked by incubation in

0.3% H_2O_2 for 5 min. The primary antibody was detected using the VECTASTAIN ABC kit (Vector Laboratories, Burlingame, CA, USA). Slides were lightly counterstained with hematoxylin.

Flow cytometry

Cells were trypsinized, fixed in 70% ethanol and then stained with propidium iodide (Sigma). Cells were passed through a FACSCalibur instrument (BD Biosciences, Billerica, MA, USA).

Microarray analysis

Expression data of cells infected with a lentivirus expressing an shRNA targeting ALK or pleiotrophin were generated using HG-U133 plus 2.0 GeneChips (Affymetrix, Santa Clara, CA, USA). Normalization and analysis of the data were conducted using Gene Spring version 11.5.1 (Agilent Technologies, Santa Clara, CA, USA). Affimetrix CEL files were uploaded to GeneSpring, and RobustMulti-Array normalization was performed. Genes downregulated >1.9-fold by ALK knockdown and those downregulated >2.3-fold by pleiotrophin knockdown were termed 'ALK_signature (ALK-sig)' and 'pleiotrophin (PTN) signature (PTN-sig)' genes, respectively (the gene lists are provided in Supplementary Tables S2 and S3). BENPORATH_ES_1 were taken from the Molecular Signature Database (MSigDB).[25,47] The Kim_Myc_module was taken from Myc human module listed in Supplementary Table S3 of Kim *et al.*[27] The significance of the overlap between sh-ALK, sh-PTN#1, BENPORATH_ES_1 and/or Kim_Myc_module was calculated by the hypergeometric distribution shown in Supplementary Table S4 (Tavazoie *et al.*[48]) Functional characterization of these genes was performed using SPEED.[49] The data derived from microarray analysis has been deposited in the Gene Expression Omnibus database (GSE32482). The expression profiles of *pleiotrophin* and *SOX2* in patient glioblastomas, two GSC lines and glioma cell lines were taken from GSE4536 (Lee *et al.*[3]).

Reporter assay

Cells were transfected with a luciferase-reporter plasmid. For *in vitro* differentiation, fetal bovine serum was added to culture medium at a final concentration of 20% and cultured for an additional 24 h. Cells were lysed and firefly luciferase activity was measured with the Luciferase Reporter Assay System (Promega) and shown as the average of three measurements.

Chromatin immunoprecipitation

Cells were fixed with 1% formalin and then the reaction was stopped by the addition of glycine to a final concentration of 125 mM. Cells were lysed in chromatin immunoprecipitated lysis buffer (50 mM Tris-HCl, pH 8.0, 1% SDS, 10 mM EDTA and protease inhibitors). Lysates were sonicated to generate DNA fragments of ~1 kb in length and then diluted 10-fold to reduce the concentration of SDS to 0.1%. Immunoprecipitations were performed with an anti-SOX2 antibody. Samples were washed, reverse-crosslinked and digested by proteinase K. Purified DNA samples were analyzed by real-time PCR, and differences in the DNA content between the bound and input fractions were determined. Primers used for amplification of the gene promoters or enhancer were as follows: *pleiotrophin* forward (5′-CAGCTCTCGAGTGCAAAGC-3′), *pleiotrophin* reverse (5′-AATGGGAGGGATGAGAGGAG-3′); *GAPDH* forward (5′-TGCGTGCCCAGTT GAACCAG-3′), *GAPDH* reverse (5′-AACAGGAGGAGCAGAGAGCGAAGC-3′); *SOX2* forward (5′-TGAAGACAGTCTAGTGGGAGATGT-3′), and *SOX2* reverse (5′-CTCTTTGGCCCAGGAAACT-3′).

CONFLICT OF INTEREST

The authors declare no conflict of interest.

ACKNOWLEDGEMENTS

This work was supported by the Research Program of Innovative Cell Biology by Innovative Technology (Integrated Systems Analysis of Cellular Oncogenic Signaling Networks), Grants-in-Aid for Scientific Research on Innovative Areas (Integrative Research on Cancer Microenvironment Network), Takeda Science Foundation and, in part, by Global COE Program (Integrative Life Science Based on the Study of Biosignaling Mechanisms), MEXT, Japan.

REFERENCES

1 Furnari FB, Fenton T, Bachoo RM, Mukasa A, Stommel JM, Stegh A *et al.* Malignant astrocytic glioma: genetics, biology, and paths to treatment. *Genes Dev* 2007; **21**: 2683–2710.
2 Chen J, McKay RM, Parada LF. Malignant glioma: lessons from genomics, mouse models, and stem cells. *Cell* 2012; **149**: 36–47.
3 Lee J, Kotliarova S, Kotliarov Y, Li A, Su Q, Donin NM *et al.* Tumor stem cells derived from glioblastomas cultured in bFGF and EGF more closely mirror the phenotype and genotype of primary tumors than do serum-cultured cell lines. *Cancer Cell* 2006; **9**: 391–403.
4 Sell S. Cancer stem cells and differentiation therapy. *Tumour Biol* 2006; **27**: 59–70.
5 Zhang J, Yang PL, Gray NS. Targeting cancer with small molecule kinase inhibitors. *Nat Rev Cancer* 2009; **9**: 28–39.
6 Kadomatsu K, Muramatsu T. Midkine and pleiotrophin in neural development and cancer. *Cancer Lett* 2004; **204**: 127–143.
7 Palmer RH, Vernersson E, Grabbe C, Hallberg B. Anaplastic lymphoma kinase: signalling in development and disease. *Biochem J* 2009; **420**: 345–361.
8 Turner SD, Alexander DR. What have we learnt from mouse models of NPM-ALK-induced lymphomagenesis? *Leukemia* 2005; **19**: 1128–1134.
9 Camidge DR, Doebele RC. Treating ALK-positive lung cancer--early successes and future challenges. *Nat Rev Clin Oncol* 2012; **9**: 268–277.
10 Gandhi L, Janne PA. Crizotinib for ALK-rearranged non-small cell lung cancer: a new targeted therapy for a new target. *Clin Cancer Res* 2012; **18**: 3737–3742.
11 Stylianou DC, Auf der Maur A, Kodack DP, Henke RT, Hohn S, Toretsky JA *et al.* Effect of single-chain antibody targeting of the ligand-binding domain in the anaplastic lymphoma kinase receptor. *Oncogene* 2009; **28**: 3296–3306.
12 Yuan H, Corbi N, Basilico C, Dailey L. Developmental-specific activity of the FGF-4 enhancer requires the synergistic action of Sox2 and Oct-3. *Genes Dev* 1995; **9**: 2635–2645.
13 Avilion AA, Nicolis SK, Pevny LH, Perez L, Vivian N, Lovell-Badge R. Multipotent cell lineages in early mouse development depend on SOX2 function. *Genes Dev* 2003; **17**: 126–140.
14 Sarkar A, Hochedlinger K. The Sox family of transcription factors: versatile regulators of stem and progenitor cell fate. *Cell Stem Cell* 2013; **12**: 15–30.
15 Episkopou V. SOX2 functions in adult neural stem cells. *Trends Neurosci* 2005; **28**: 219–221.
16 Schmitz M, Temme A, Senner V, Ebner R, Schwind S, Stevanovic S *et al.* Identification of SOX2 as a novel glioma-associated antigen and potential target for T cell-based immunotherapy. *Br J Cancer* 2007; **96**: 1293–1301.
17 Gangemi RM, Griffero F, Marubbi D, Perera M, Capra MC, Malatesta P *et al.* SOX2 silencing in glioblastoma tumor-initiating cells causes stop of proliferation and loss of tumorigenicity. *Stem Cells* 2009; **27**: 40–48.
18 Lottaz C, Beier D, Meyer K, Kumar P, Hermann A, Schwarz J *et al.* Transcriptional profiles of CD133+ and CD133- glioblastoma-derived cancer stem cell lines suggest different cells of origin. *Cancer Res* 2010; **70**: 2030–2040.
19 Koyama-Nasu R, Nasu-Nishimura Y, Todo T, Ino Y, Saito N, Aburatani H *et al.* The critical role of cyclin D2 in cell cycle progression and tumorigenicity of glioblastoma stem cells. *Oncogene* (e-pub ahead of print 10 September 2012; doi:10.1038/onc.2012.399).
20 Mizrak D, Brittan M, Alison M. CD133: molecule of the moment. *J Pathol* 2008; **214**: 3–9.
21 Barker N, van Es JH, Kuipers J, Kujala P, van den Born M, Cozijnsen M *et al.* Identification of stem cells in small intestine and colon by marker gene Lgr5. *Nature* 2007; **449**: 1003–1007.
22 Wurdak H, Zhu S, Romero A, Lorger M, Watson J, Chiang CY *et al.* An RNAi screen identifies TRRAP as a regulator of brain tumor-initiating cell differentiation. *Cell Stem Cell* 2010; **6**: 37–47.
23 Powers C, Aigner A, Stoica GE, McDonnell K, Wellstein A. Pleiotrophin signaling through anaplastic lymphoma kinase is rate-limiting for glioblastoma growth. *J Biol Chem* 2002; **277**: 14153–14158.
24 Galli R, Binda E, Orfanelli U, Cipelletti B, Gritti A, De Vitis S *et al.* Isolation and characterization of tumorigenic, stem-like neural precursors from human glioblastoma. *Cancer Res* 2004; **64**: 7011–7021.
25 Ben-Porath I, Thomson MW, Carey VJ, Ge R, Bell GW, Regev A *et al.* An embryonic stem cell-like gene expression signature in poorly differentiated aggressive human tumors. *Nat Genet* 2008; **40**: 499–507.
26 Raetz EA, Perkins SL, Carlson MA, Schooler KP, Carroll WL, Virshup DM. The nucleophosmin-anaplastic lymphoma kinase fusion protein induces c-Myc expression in pediatric anaplastic large cell lymphomas. *Am J Pathol* 2002; **161**: 875–883.
27 Kim J, Woo AJ, Chu J, Snow JW, Fujiwara Y, Kim CG *et al.* A Myc network accounts for similarities between embryonic stem and cancer cell transcription programs. *Cell* 2010; **143**: 313–324.
28 Singh SK, Hawkins C, Clarke ID, Squire JA, Bayani J, Hide T *et al.* Identification of human brain tumour initiating cells. *Nature* 2004; **432**: 396–401.

29 Parsons DW, Jones S, Zhang X, Lin JC, Leary RJ, Angenendt P *et al.* An integrated genomic analysis of human glioblastoma multiforme. *Science* 2008; **321**: 1807–1812.
30 Cancer Genome Atlas Research Network. Comprehensive genomic characterization defines human glioblastoma genes and core pathways. *Nature* 2008; **455**: 1061–1068.
31 Ying M, Wang S, Sang Y, Sun P, Lal B, Goodwin CR *et al.* Regulation of glioblastoma stem cells by retinoic acid: role for Notch pathway inhibition. *Oncogene* 2011; **30**: 3454–3467.
32 Carpenter EL, Mosse YP, Targeting ALK. in neuroblastoma--preclinical and clinical advancements. *Nat Rev Clin Oncol* 2012; **9**: 391–399.
33 Dirks WG, Fahnrich S, Lis Y, Becker E, MacLeod RA, Drexler HG. Expression and functional analysis of the anaplastic lymphoma kinase (ALK) gene in tumor cell lines. *Int J Cancer* 2002; **100**: 49–56.
34 Meng K, Rodriguez-Pena A, Dimitrov T, Chen W, Yamin M, Noda M *et al.* Pleiotrophin signals increased tyrosine phosphorylation of β-catenin through inactivation of the intrinsic catalytic activity of the receptor-type protein tyrosine phosphatase beta/zeta. *Proc Natl Acad Sci USA* 2000; **97**: 2603–2608.
35 Raulo E, Chernousov MA, Carey DJ, Nolo R, Rauvala H. Isolation of a neuronal cell surface receptor of heparin binding growth-associated molecule (HB-GAM). Identification as N-syndecan (syndecan-3). *J Biol Chem* 1994; **269**: 12999–13004.
36 Perez-Pinera P, Chang Y, Deuel TF. Pleiotrophin, a multifunctional tumor promoter through induction of tumor angiogenesis, remodeling of the tumor microenvironment, and activation of stromal fibroblasts. *Cell Cycle* 2007; **6**: 2877–2883.
37 Bernhardt M, Galach M, Novak D, Utikal J. Mediators of induced pluripotency and their role in cancer cells—current scientific knowledge and future perspectives. *Biotechnol J* 2012; **7**: 810–821.
38 Chen S, Xu Y, Chen Y, Li X, Mou W, Wang L *et al.* SOX2 gene regulates the transcriptional network of oncogenes and affects tumorigenesis of human lung cancer cells. *PLoS One* 2012; **7**: e36326.
39 Leis O, Eguiara A, Lopez-Arribillaga E, Alberdi MJ, Hernandez-Garcia S, Elorriaga K *et al.* Sox2 expression in breast tumours and activation in breast cancer stem cells. *Oncogene* 2012; **31**: 1354–1365.
40 Kondo T, Raff M. Chromatin remodeling and histone modification in the conversion of oligodendrocyte precursors to neural stem cells. *Genes Dev* 2004; **18**: 2963–2972.
41 Ferri AL, Cavallaro M, Braid D, Di Cristofano A, Canta A, Vezzani A *et al.* Sox2 deficiency causes neurodegeneration and impaired neurogenesis in the adult mouse brain. *Development* 2004; **131**: 3805–3819.
42 Cavallaro M, Mariani J, Lancini C, Latorre E, Caccia R, Gull F *et al.* Impaired generation of mature neurons by neural stem cells from hypomorphic Sox2 mutants. *Development* 2008; **135**: 541–557.
43 McDermott U, lafrate AJ, Gray NS, Shioda T, Classon M, Maheswaran S *et al.* Genomic alterations of anaplastic lymphoma kinase may sensitize tumors to anaplastic lymphoma kinase inhibitors. *Cancer Res* 2008; **68**: 3389–3395.
44 Amet LE, Lauri SE, Hienola A, Croll SD, Lu Y, Levorse JM *et al.* Enhanced hippocampal long-term potentiation in mice lacking heparin-binding growth-associated molecule. *Mol Cell Neurosci* 2001; **17**: 1014–1024.
45 Hienola A, Pekkanen M, Raulo E, Vanttola P, Rauvala H. HB-GAM inhibits proliferation and enhances differentiation of neural stem cells. *Mol Cell Neurosci* 2004; **26**: 75–88.
46 Melosky B. Supportive care treatments for toxicities of anti-egfr and other targeted agents. *Curr Oncol* 2012; **19**: S59–S63.
47 Subramanian A, Tamayo P, Mootha VK, Mukherjee S, Ebert BL, Gillette MA *et al.* Gene set enrichment analysis: a knowledge-based approach for interpreting genome-wide expression profiles. *Proc Natl Acad Sci USA* 2005; **102**: 15545–15550.
48 Tavazoie S, Hughes JD, Campbell MJ, Cho RJ, Church GM. Systematic determination of genetic network architecture. *Nat Genet* 1999; **22**: 281–285.
49 Parikh JR, Klinger B, Xia Y, Marto JA, Bluthgen N. Discovering causal signaling pathways through gene-expression patterns. *Nucleic Acids Res* 2010; **38**: W109–W117.
50 Chew JL, Loh YH, Zhang W, Chen X, Tam WL, Yeap LS *et al.* Reciprocal transcriptional regulation of Pou5f1 and Sox2 via the Oct4/Sox2 complex in embryonic stem cells. *Mol Cell Biol* 2005; **25**: 6031–6046.

Supplementary Information accompanies this paper on the Oncogene website (http://www.nature.com/onc)

Biochemical and Biophysical Research Communications 444 (2014) 13–18

Contents lists available at ScienceDirect

Biochemical and Biophysical Research Communications

journal homepage: www.elsevier.com/locate/ybbrc

PCDH10 is required for the tumorigenicity of glioblastoma cells

Kanae Echizen [a], Mitsutoshi Nakada [b,*], Tomoatsu Hayashi [a], Hemragul Sabit [b], Takuya Furuta [b], Miyuki Nakai [a], Ryo Koyama-Nasu [a], Yukiko Nishimura [a], Kenzui Taniue [a], Yasuyuki Morishita [c], Shinji Hirano [d], Kenta Terai [e], Tomoki Todo [f], Yasushi Ino [f], Akitake Mukasa [f], Shunsaku Takayanagi [f], Ryohei Ohtani [f], Nobuhito Saito [f], Tetsu Akiyama [a,*]

[a] Laboratory of Molecular and Genetic Information, Institute of Molecular and Cellular Biosciences, The University of Tokyo, 1-1-1, Yayoi, Bunkyo-ku, Tokyo 113-0032, Japan
[b] Department of Neurosurgery, Graduate School of Medical Science, Kanazawa University, 13-1, Takara-machi, Kanazawa 920-8641, Japan
[c] Department of Molecular Pathology, Graduate School of Medicine, The University of Tokyo, 7-3-1, Hongo, Bunkyo-ku, Tokyo 113-0033, Japan
[d] Department of Neurobiology and Anatomy, Kochi Medical School, Kochi University, Okoh-cho, Nangoku-City, Kochi 783-8505, Japan
[e] Laboratory of Function and Morphology, Institute of Molecular and Cellular Biosciences, The University of Tokyo, 1-1-1, Yayoi, Bunkyo-ku, Tokyo 113-0032, Japan
[f] Department of Neurosurgery, Faculty of Medicine, The University of Tokyo, 7-3-1, Hongo, Bunkyo-ku, Tokyo 113-8655, Japan

ARTICLE INFO

Article history:
Received 19 December 2013
Available online 6 January 2014

Keywords:
Protocadherin PCDH10
OL-protocadherin
Glioblastoma
Tumorigenicity
Proliferation

ABSTRACT

Protocadherin10 (PCDH10)/OL-protocadherin is a cadherin-related transmembrane protein that has multiple roles in the brain, including facilitating specific cell–cell connections, cell migration and axon guidance. It has recently been reported that PCDH10 functions as a tumor suppressor and that its overexpression inhibits proliferation or invasion of multiple tumor cells. However, the function of PCDH10 in glioblastoma cells has not been elucidated. In contrast to previous reports on other tumors, we show here that suppression of the expression of PCDH10 by RNA interference (RNAi) induces the growth arrest and apoptosis of glioblastoma cells *in vitro*. Furthermore, we demonstrate that knockdown of PCDH10 inhibits the growth of glioblastoma cells xenografted into immunocompromised mice. These results suggest that PCDH10 is required for the proliferation and tumorigenicity of glioblastoma cells. We speculate that PCDH10 may be a promising target for the therapy of glioblastoma.

1. Introduction

Protocadherin10 (PCDH10)/OL-protocadherin is a transmembrane protein that has 6 cadherin domains in the extra cellular region and belongs to the δ2-protocadherin family of proteins [1–3]. PCDH10 is concentrated at cell–cell junctions and promotes aggregation, although its aggregative strength is weaker than that of classical cadherins [4]. Furthermore, PCDH10 recruits the Nap1-WAVE complex at the sites of cell–cell contact and promotes reorganization of the actin cytoskeleton, which results in accelerated cell migration on confluent cell monolayers [5]. In neuronal cells, PCDH10 is localized along the axons, is concentrated in the growth cones and is involved in axon guidance [5,6].

It has recently been reported that CpG islands within PCDH10 are highly methylated and epigenetically silenced in many tumors, including breast cancer, nasopharyngeal, esophageal carcinoma and haematological malignancies and this is associated with poor prognosis [7–12]. It has also been reported that overexpression of PCDH10 significantly inhibits proliferation or invasion of multiple tumor cells *in vitro* [9,11].

Glioblastoma is a highly invasive and progressive tumor type, with an overall 5-year survival rate of less than 5% [13]. In the present study, we examined whether PCDH10 also exerts a tumor suppressive function in glioblastoma cells. We unexpectedly found that PCDH10 is required for the proliferation and tumorigenicity of glioblastoma cells.

2. Materials and methods

2.1. Cell lines and tumor specimens

Following informed consent, tumor samples classified as primary glioblastoma were obtained from patients undergoing surgical treatment at Kanazawa University Hospital and the University of Tokyo Hospital as approved by the Institutional Review Board. The human astrocytoma cell lines U87, U251, T98G and LN229 (ATCC) were cultured in DMEM (GIBCO) supplemented with 10% fetal bovine serum. Cell lines GB1~16 were cultured in DMEM/F-12 containing B27 supplement (GIBCO), EGF and FGF2 (20 ng/ml each, Wako) on laminin-coated culture dishes [14–16].

* Corresponding authors. Fax: +81 76 234 4262 (M. Nakada), +81 3 5841 8482 (T. Akiyama).
E-mail addresses: mnakada@med.kanazawa-u.ac.jp (M. Nakada), akiyama@iam.u-tokyo.ac.jp (T. Akiyama).

0006-291X/$ - see front matter © 2014 Elsevier Inc. All rights reserved.
http://dx.doi.org/10.1016/j.bbrc.2013.12.138

2.2. Antibodies

Mouse monoclonal antibody (mAb) to PCDH10 (5G10) was prepared as described previously [6]. mAbs to α-tubulin, Flag M2 and Ki67 were purchased from CALBIOCHEM, Sigma–Aldrich and Leica Biosystems, respectively. Rabbit polyclonal antibody to GFP was from Santa Cruz.

2.3. Immunohistochemistry

Formalin-fixed and paraffin-embedded tissue blocks were sectioned (6 μm thick) onto slides and then deparaffinized. Slides were microwaved for 15 min in target retrieval solution (pH 6.0; Dako). Internal peroxidases were blocked by incubation in 0.3% H_2O_2 solution in methanol for 20 min. Non-specific staining was blocked by a 30 min incubation with blocking solution (5% skim milk, 0.1% Tween20 in TBS). Sections were immunostained with the ABC kit (VECTOR). Anti-PCDH10 (5G10), anti-Ki67 and anti-GFP antibodies were used at a dilution of 1:200. Sections were exposed to diaminobenzidine peroxidase substrate (Funakoshi) for 5–10 min and counterstained with Mayer's hematoxylin. Non-immune rat IgG was used as a negative control. All images were taken by bright field microscopy AX80 (Olympus). Ki67 index was calculated as the number of Ki67-positive cells per 1.0×10^3 cells in each of 6 fields per sample.

2.4. Lentivirus production

The entry vector pENTRH1 (obtained from K. Ui-Tei), the lentiviral vector CS-RfA-CG and the packaging vectors pCAG-HIV-gp and pCMV-VSV-G-RSV-Rev (provided by H. Miyoshi) were used for lentivirus production. The target sequences for shRNA are as follows: luciferase, 5′-GATTTCGAGTCGTCTTAATGT-3′; DsRed, 5′-GCCCCGT AATGCAGAAGAAGA-3′; human PCDH10#2, 5′-GTGCGTGGCAAC-GAAATGAAC-3′; human PCDH10#4, 5′-GAGAAGAAGCTCAACATC-TAT-3′. Infection efficiency was monitored by GFP expression driven by the CMV promoter.

2.5. Single-cell migration assay

Time-lapse images were obtained at 5-min intervals for 4 h using a microscope (IX81; Olympus) equipped with a cooled CCD camera CoolSNAP K4 (Photometrics). GB2 cells (1×10^3 cells) infected with shRNA-expressing lentiviruses for 3 days (MOI = 6) were plated on laminin-coated, glass-bottom, 24-well plates (Iwaki) and GFP signals were traced. Trace drawing and statistical analyses were performed with IMARIS Track (BitPlane) and Excel (Microsoft), respectively. The box plots were presented as described previously [5].

2.6. In vitro invasion assay

In vitro invasion assays were performed using 24-well Biocoat Matrigel invasion chambers (BD Biosciences). GB2 cells (1.0×10^5 cells per well) infected with shRNA-expressing viruses for 4 days (MOI = 3) were starved overnight with DMEM/F-12 medium and allowed to migrate toward the underside of the top chamber for 24 h. The lower chamber was filled with DMEM/F12 containing 10% FBS. Cells in the top chamber were removed and the number of infiltrated cells was counted by Cell Titer-Glo assays. Infiltrated cells were fixed with methanol and subjected to HE staining (Merck).

2.7. Cell proliferation assay

Cell viability was determined using the Cell Titer-Glo Luminescent Cell Viability Assay kit (Promega). Luminescence was measured on a Mithras LB 940 (Berthold).

2.8. Pcdh10

The full-length *PCDH10* variant 1 cDNA (obtained from Q. Tao) was subcloned into the pIRES hrGFP 3 × Flag vector (Adgilent). 3 × Flag tagged PCDH10 was subcloned into the pENTR4 dual selection vector (Invitrogen).

2.9. Apoptosis assay

Apoptotic cells were detected using the Annexin V-Biotin Apoptosis Detection Kit (MBL) and labeled with Streptavidin-APC conjugates (S888, Invitrogen). A minimum of 5×10^3 cells were analyzed with flow cytometer Canto II (BD Bioscience) and FlowJo 8.8.7 software (TreeStar, Ashland, OR).

2.10. Sphere formation assay

GB2 cells infected with shRNA-expressing lentiviruses (MOI = 3) for 3 days were plated on 96-well tissue culture plates (1000, 500 or 250 cells per well) and cultured for 2 weeks. Spheres were photographed by In Cell Analyzer 2000 (GE Healthcare) and analyzed by Developer 1.9.1 software (GE Healthcare).

2.11. Real time PCR

Real time PCR was performed as described previously [14]. The results were normalized to the detected values for GAPDH. Primer sequences are as follows: PCDH10 sense, 5′-AGGCCCTTCACAG-CACTCT-3′; antisense, 5′-GACTAGCATATCCTTTTCCGTGTC-3′; GAP-DH sense, 5′-TGGTGAAGACGCCAGTGGA-3′; antisense, 5′-GCACCGTCAAGGCTGAGAAC-3′.

Immunoblotting analysis and tumor formation assays were performed as described previously [14].

3. Results and discussion

3.1. PCDH10 is expressed in glioblastoma cells

We established eight glioblastoma cell lines under serum-free conditions [14–16]. These cell lines retained clonogenic potential and were highly tumorigenic when transplanted into immunocompromised mice. Immunoblotting analysis with anti-PCDH10 antibody revealed that most of these cell lines expressed substantial levels of PCDH10 protein (Fig. 1A), in contrast to previous reports showing weak or no expression in many other tumor types. In particular, PCDH10 was abundantly expressed in GB2 and GB3 cells. By contrast, PCDH10 was not expressed at detectable levels in four commonly used glioblastoma cell lines, LN229, T98G, U251 and U87MG, which are cultured in serum-containing medium. Furthermore, immunohistochemical analysis showed that 11 out of 19 patient specimens (57.9%) were positive for PCDH10 (Fig. 1B and Supplementary Table 1). In addition, we found that PCDH10 was expressed in neurons but not in astrocytes or oligodendrocytes from normal human brain (data not shown).

3.2. PCDH10 is required for glioblastoma cell migration and invasion

It has been reported that PCDH10 binds to the Nap1-Wave complex and controls the migration of U251 cells [5]. We therefore

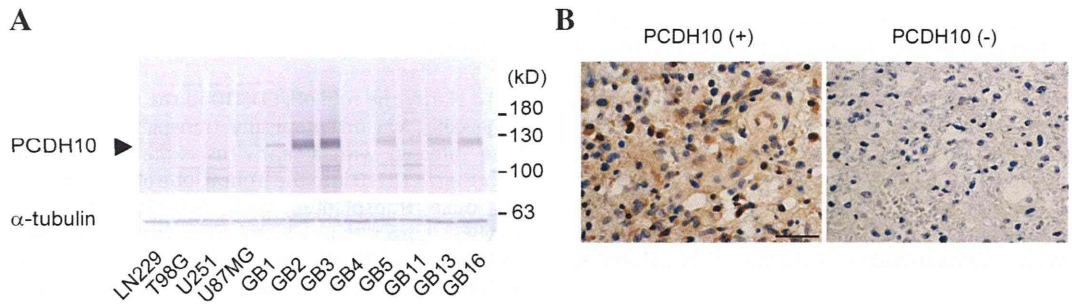

Fig. 1. Expression of PCDH10 in glioblastoma cells. (A) Lysates from glioblastoma cells were subjected to immunoblotting analysis with anti-PCDH10 antibody. LN229, T98G, U251 and U87MG were cultured in serum-containing medium, and GB1~16 cells were cultured in serum-free medium. The arrowhead indicates PCDH10. α-Tubulin was used as a control. (B) Histological examination of patients' samples. Tissue sections were stained with anti-PCDH10 antibody. Representative sections from PCDH10-positive (Left) and -negative (Right) tumors are shown. Scale bars, 20 μm.

used time-lapse microscopy to examine whether PCDH10 plays a role in migration of glioblastoma cells cultured on laminin-coated dishes. We found that infection of GB2 cells with a lentivirus expressing an shRNA targeting PCDH10 resulted in a significant decrease in cell migratory activity (sh-luciferase vs sh-PCDH10#2, $p = 0.021$; sh-luciferase vs sh-PCDH10#4, $p = 0.00059$) (Fig. 2A and B), as well as a decrease in PCDH10 protein levels (Supplementary Fig. 1), but did not affect adhesion to laminin-coated dishes (Fig. 2C). Since glioblastoma is a highly invasive tumor [13,17], we also performed Matrigel invasion assays. We found that knockdown of PCDH10 resulted in a decrease in the invasive activity of GB2 cells (sh-luciferase vs sh-PCDH10#2, $p = 0.034$; sh-luciferase vs sh-PCDH10#4, $p = 0.042$) (Fig. 2D and E). These results suggest that PCDH10 has the potential to promote migration and invasion of glioblastoma cells.

3.3. Knockdown of PCDH10 induces the growth arrest and apoptosis of glioblastoma cells

It has recently been shown that overexpression of PCDH10 inhibits the proliferation of multiple tumor cells *in vitro* [9,11]. We therefore investigated the significance of PCDH10 in the proliferation of three glioblastoma cell lines, GB2, GB3 and GB16, in which PCDH10 is abundantly expressed (Fig. 1A). Cell Titer-Glo assays revealed that infection of these cells with a lentivirus expressing an shRNA targeting PCDH10 resulted in a decrease in

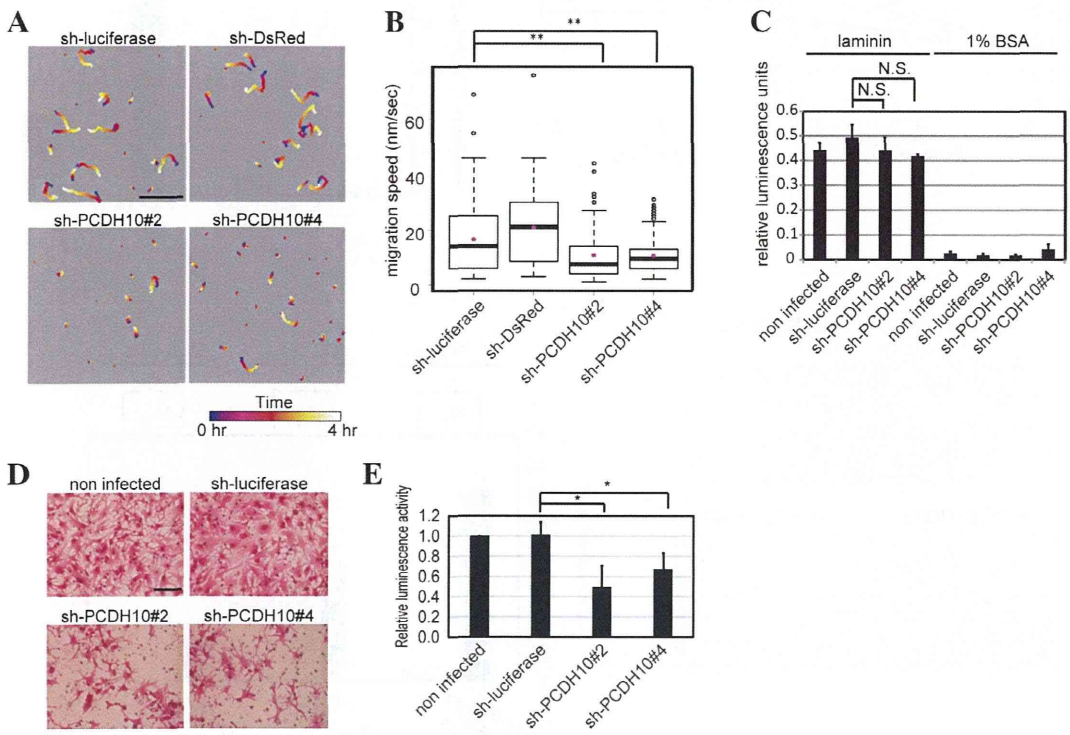

Fig. 2. PCDH10 is required for the migration and invasion of glioblastoma cells. (A and B) GB2 cells were infected with the indicated shRNA-expressing lentivirus at MOI = 6. Time-lapse images were taken at 5-min intervals for 4 h. (A) One representative field of each sample. Tracks of individual cells that neither divided nor contacted other cells were analyzed. Scale bar, 400 μm. (B) Images were taken from 9 fields per sample. The number of cells analyzed was: sh-luciferase, $n = 140$; sh-DsRed, $n = 131$; sh-PCDH10#2, $n = 138$; sh-PCDH10#4, $n = 158$. Bars indicate medians and magenta dots indicate means ($n = 4$). $^{**}p < 0.01$. (C) GB2 cells were infected with the indicated shRNA expressing lentivirus at MOI = 6. Cells were re-plated 5 days after the infection. Adherent cell numbers were determined by Cell Titer-Glo assays. Dishes coated with 1% BSA were used as controls. Results are shown as average of 4 wells ± SD. $^{*}p < 0.05$. (D and E) GB2 cells were infected with the indicated shRNA-expressing lentivirus at MOI = 3. 1.0×10^5 cells were allowed to migrate toward the underside of the top chamber for 24 h. (D) HE staining of the invaded cells. Scale bar, 100 μm. (E) Cell Titer-Glo assays of the invaded cells. Results are shown as average of 3 wells ± SD. $^{*}p < 0.05$.

their proliferation (Fig. 3A). By contrast, overexpression of PCDH10 did not affect proliferation of T98G or U251 cells, which do not express detectable levels of PCDH10 protein (Supplementary Fig. 2). We also performed AnnexinV assays and found that knockdown of PCDH10 induced apoptosis of GB2 cells (Fig. 3B and C). We next performed sphere formation assays to clarify the role of PCDH10 in the self-renewal capacity of glioblastoma cells. We found that knockdown of PCDH10 by shRNA resulted in significant inhibition of sphere formation (Fig. 3D and E). Thus, PCDH10 may be critical for the proliferation, survival and self-renewal of glioblastoma cells.

3.4. Knockdown of PCDH10 suppresses the tumorigenicity of glioblastoma cells

To clarify the role of PCDH10 in the tumorigenicity of glioblastoma cells, we orthotopically transplanted GB16 cells that had been infected with a lentivirus expressing GFP and an shRNA targeting PCDH10 into the frontal lobe of nude mice. We found that the mice transplanted with PCDH10-knockdown GB16 cells survived longer than control mice (sh PCDH10#2, log-rank test $p = 0.042$; sh PCDH10#4, log-rank test $p = 0.00031$) (Fig. 4A). Histological studies revealed that all mice transplanted with

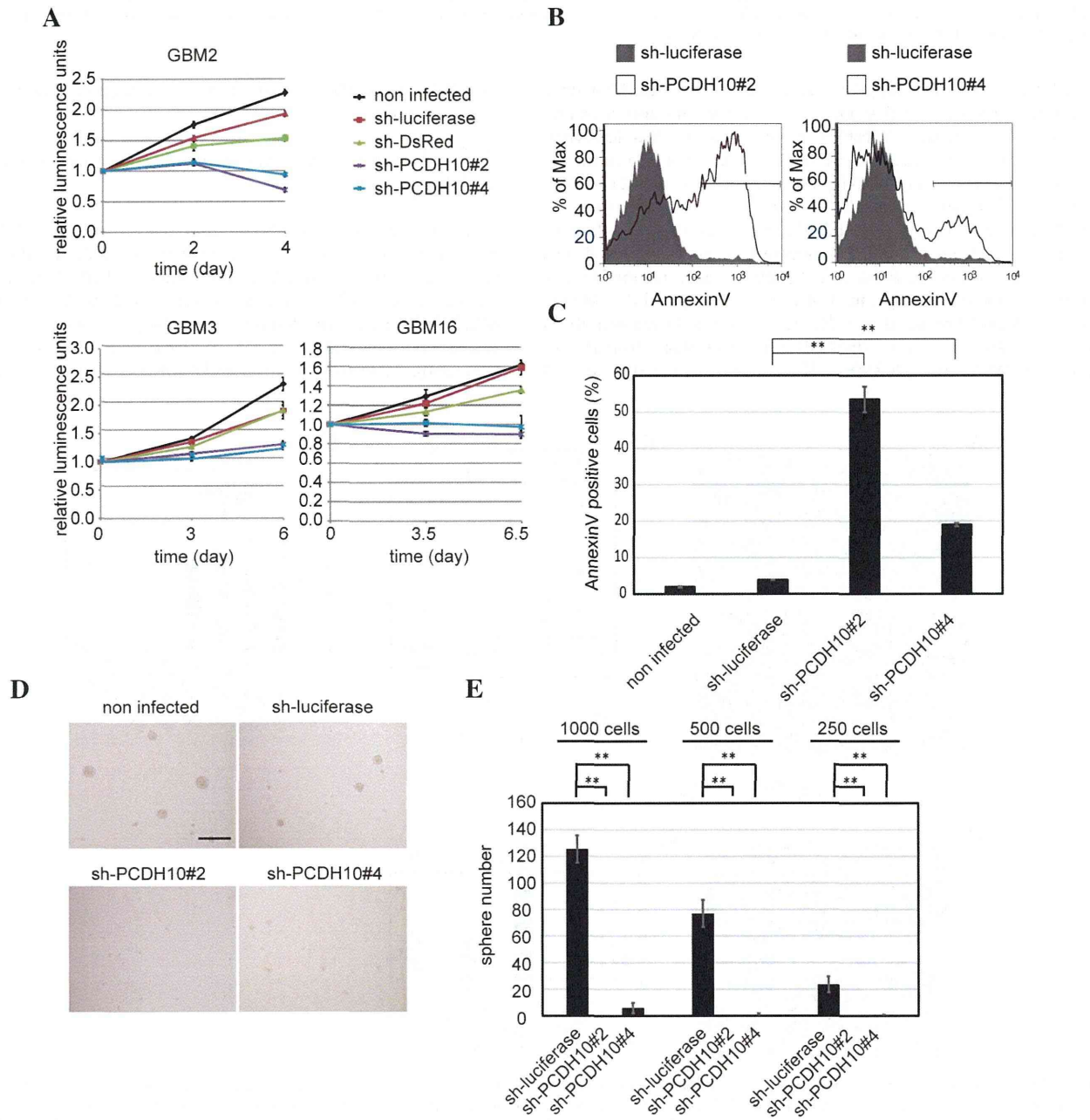

Fig. 3. PCDH10 is required for the proliferation, survival and self-renewal of glioblastoma cells. (A) Cell Titer-Glo assays were performed with GB2, GB3 or GB16 cells infected with a lentivirus expressing an shRNA targeting PCDH10 (MOI = 3). Results are shown as average of 5 wells ± SD. (B) AnnexinV assays were performed with GB2 cells that had been infected with a lentivirus expressing an shRNA targeting PCDH10 for 8 days. (C) AnnexinV-positive populations in (B) are shown. Results are shown as the mean ± SD ($n = 3$). At least 5000 cells were analyzed per sample. $^{**}p < 0.01$. (D and E) Sphere formation assays were performed with GB2 cells that had been infected with a lentivirus expressing an shRNA targeting PCDH10 for 17 days. (D) Bright field images of spheres. (E) Results are shown as average of 6 wells ± SD. $^{**}p < 0.01$.

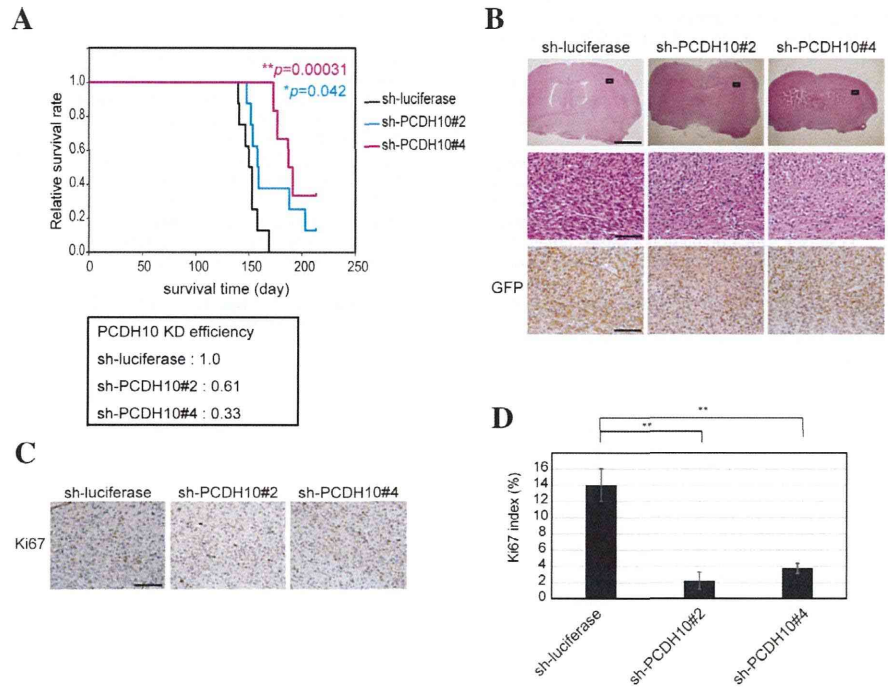

Fig. 4. PCDH10 is required for the tumorigenicity of glioblastoma cells. (A) Kaplan–Meier survival curves of mice transplanted with 1.0×10^4 GB16 cells infected with a lentivirus expressing GFP and shRNA targeting PCDH10 or luciferase (control) (MOI = 1; $n = 8$ for shPCDH10#2 and luciferase; $n = 6$ for shPCDH10#4). (B) Histological analysis of tumors harvested from the mice in (A). Tissue sections were stained with HE or anti-GFP antibody. General views (Upper Panel; Scale bar, 2.0 mm) and magnified views (Middle and Lower panels; Scale bars, 100 μm) of the region around the corpus callosum in the right hemisphere (near the injection point, black squares in the upper panel). (C and D) Immunohistochemical analysis of tumors harvested from the mice in (A). Tissue sections were stained with anti-GFP and anti-Ki-67 antibodies. Scale bars, 100 μm. (D) Ki67 indices of the brain sections. 1.0×10^3 cells were counted in each field. Results are shown as average of 6 fields ± SD. $^{**}p < 0.01$.

GB16 cells had developed tumors with diffuse infiltration into surrounding brain tissues, one of the hallmark features of glioblastoma (Fig. 4B). The density of GFP-expressing cells (injected tumor cells) was slightly lower in the brains of the mice transplanted with PCDH10-knockdown GB16 cells compared to those of control mice (Fig. 4B). Furthermore, we observed that the number of Ki67-positive cells was significantly reduced in the brains of the mice transplanted with PCDH10-knockdown GB16 cells compared to those of control mice (sh-luciferase, 14.0 ± 2.0%; sh-PCDH10#2, 2.2 ± 1.1%; sh-PCDH10#4, 3.7 ± 0.64%) (Fig. 4C and D). These results suggest that knockdown of PCDH10 suppresses the proliferation of glioblastoma cells and extends the survival of tumor-bearing mice.

These results show that PCDH10 is required for the proliferation and tumorigenicity of glioblastoma cells. This suggests that PCDH10 may function differently at the molecular level in glioblastoma cells compared to other tumor cell types. This may mean that PCDH10 associates with different molecules and elicits different downstream signals in glioblastoma cells than it does in other tumor cells. The molecular mechanisms underlying this functional difference remain to be elucidated. It also remains to be investigated whether PCDH10 expression levels are associated with the classification and prognosis of glioblastoma patients. Finally, we speculate that PCDH10 may be a potential therapeutic target for glioblastoma. In particular, monoclonal antibodies that target the extracellular domain of PCDH10 could hold promise as novel anti-tumor reagents.

Acknowledgments

This work was supported by Research Program of Innovative Cell Biology by Innovative Technology (Integrated Systems Analysis of Cellular Oncogenic Signaling Networks), Grants-in-Aid for Scientific Research on Innovative Areas (Integrative Research on Cancer Microenvironment Network), Project for Development of Innovative Research on Cancer Therapeutics, Grant-in-Aid for Scientific Research (C-23592117) from the Japan Society for the Promotion of Science (M. Nakada) and Foundation for Promotion of Cancer Research (M. Nakada), Takeda Science Foundation, Kato Memorial Bioscience Foundation and in part by Global COE Program (Integrative Life Science Based on the Study of Biosignaling Mechanisms), MEXT, Japan.

Appendix A. Supplementary data

Supplementary data associated with this article can be found, in the online version, at http://dx.doi.org/10.1016/j.bbrc.2013.12.138.

References

[1] Q. Wu, T. Maniatis, A striking organization of a large family of human neural cadherin-like cell adhesion genes, Cell 97 (1999) 779–790.
[2] S. Hirano, M. Takeichi, Cadherins in brain morphogenesis and wiring, Physiol. Rev. 92 (2011) 597–634.
[3] W.V. Chen, T. Maniatis, Clustered protocadherins, Development 140 (2013) 3297–3302.
[4] S. Hirano, Q. Yan, S.T. Suzuki, Expression of a novel protocadherin, OL-protocadherin, in a subset of functional systems of the developing mouse brain, J. Neurosci. 19 (1999) 995–1005.
[5] S. Nakao, A. Platek, S. Hirano, M. Takeichi, Contact-dependent promotion of cell migration by the OL-protocadherin-Nap1 interaction, J. Cell Biol. 182 (2008) 395–410.
[6] M. Uemura, S. Nakao, S.T. Suzuki, M. Takeichi, S. Hirano, OL-protocadherin is essential for growth of striatal axons and thalamocortical projections, Nat. Neurosci. 10 (2007) 1151–1159.
[7] K. Miyamoto, T. Fukutomi, S. Akashi-Tanaka, T. Hasegawa, T. Asahara, T. Sugimura, T. Ushijima, Identification of 20 genes aberrantly methylated in human breast cancers, Int. J. Cancer 116 (2005) 407–414.
[8] J. Ying, H. Li, T.J. Seng, C. Langford, G. Srivastava, S.W. Tsao, T. Putti, P. Murray, A.T. Chan, Q. Tao, Functional epigenetics identifies a protocadherin PCDH10 as a candidate tumor suppressor for nasopharyngeal, esophageal and multiple other carcinomas with frequent methylation, Oncogene 25 (2006) 1070–1080.

[9] X. Zhong, Y. Zhu, J. Mao, J. Zhang, S. Zheng, Frequent epigenetic silencing of PCDH10 by methylation in human colorectal cancer, J. Cancer Res. Clin. Oncol. 139 (2013) 485–490.
[10] J. Ying, Z. Gao, H. Li, G. Srivastava, P.G. Murray, H.K. Goh, C.Y. Lim, Y. Wang, T. Marafioti, D.Y. Mason, R.F. Ambinder, A.T. Chan, Q. Tao, Frequent epigenetic silencing of protocadherin 10 by methylation in multiple haematologic malignancies, Br. J. Haematol. 136 (2007) 829–832.
[11] J. Yu, Y.Y. Cheng, Q. Tao, K.F. Cheung, C.N. Lam, H. Geng, L.W. Tian, Y.P. Wong, J.H. Tong, J.M. Ying, H. Jin, K.F. To, F.K. Chan, J.J. Sung, Methylation of protocadherin 10, a novel tumor suppressor, is associated with poor prognosis in patients with gastric cancer, Gastroenterology 136 (2009). 640–651 e641.
[12] J.G. Ma, Z.K. He, J.H. Ma, W.P. Li, G. Sun, Downregulation of protocadherin-10 expression correlates with malignant behaviour and poor prognosis in human bladder cancer, J. Int. Med. Res. 41 (2013) 38–47.
[13] J. Chen, R.M. McKay, L.F. Parada, Malignant glioma: lessons from genomics, mouse models, and stem cells, Cell 149 (2012) 36–47.
[14] R. Koyama-Nasu, Y. Nasu-Nishimura, T. Todo, Y. Ino, N. Saito, H. Aburatani, K. Funato, K. Echizen, H. Sugano, R. Haruta, M. Matsui, R. Takahashi, E. Manabe, T. Oda, T. Akiyama, The critical role of cyclin D2 in cell cycle progression and tumorigenicity of glioblastoma stem cells, Oncogene 32 (2013) 3840–3845.
[15] J. Lee, S. Kotliarova, Y. Kotliarov, A. Li, Q. Su, N.M. Donin, S. Pastorino, B.W. Purow, N. Christopher, W. Zhang, J.K. Park, H.A. Fine, Tumor stem cells derived from glioblastomas cultured in bFGF and EGF more closely mirror the phenotype and genotype of primary tumors than do serum-cultured cell lines, Cancer Cell 9 (2006) 391–403.
[16] S.M. Pollard, K. Yoshikawa, I.D. Clarke, D. Danovi, S. Stricker, R. Russell, J. Bayani, R. Head, M. Lee, M. Bernstein, J.A. Squire, A. Smith, P. Dirks, Glioma stem cell lines expanded in adherent culture have tumor-specific phenotypes and are suitable for chemical and genetic screens, Cell Stem Cell 4 (2009) 568–580.
[17] M. Nakada, S. Nakada, T. Demuth, N.L. Tran, D.B. Hoelzinger, M.E. Berens, Molecular targets of glioma invasion, Cell. Mol. Life Sci. 64 (2007) 458–478.

OPEN ACCESS Freely available online

PLOS ONE

Identification of Two Wnt-Responsive Elements in the Intron of RING Finger Protein 43 (RNF43) Gene

Norihiko Takahashi, Kiyoshi Yamaguchi, Tsuneo Ikenoue, Tomoaki Fujii, Yoichi Furukawa*

Division of Clinical Genome Research, Advanced Clinical Research Center, Institute of Medical Science, The University of Tokyo, Tokyo, Japan

Abstract

RING finger protein 43 (RNF43), an E3-type ubiquitin ligase, is frequently up-regulated in human colorectal cancer. It has been shown that expression of *RNF43* is regulated by the Wnt-signaling pathway. However the regulatory region(s) for its transcriptional activation has not been clarified. In this study, we have shown for the first time that *RNF43* is a direct target of TCF4/β-catenin complex, and that its expression is regulated by a regulatory region containing two Wnt-responsive elements (WREs) in intron2. A reporter gene assay revealed that nucleotide substitutions in the WREs decreased the reporter activity in colon cancer cells, suggesting that both WREs are involved in the transcriptional activation. Knockdown of β-catenin by siRNA suppressed the reporter activity. In addition, ChIP assay showed that both elements associate with TCF4/β-catenin complex in colon cancer cells. These data indicate that expression of *RNF43* is regulated by the canonical Wnt/β-catenin pathway through binding of the WREs with TCF4/β-catenin complex. These findings should be useful for the understanding of the regulatory mechanism of RNF43 and may contribute to the clarification of signaling pathways regulated by RNF43.

Citation: Takahashi N, Yamaguchi K, Ikenoue T, Fujii T, Furukawa Y (2014) Identification of Two Wnt-Responsive Elements in the Intron of RING Finger Protein 43 (RNF43) Gene. PLoS ONE 9(1): e86582. doi:10.1371/journal.pone.0086582

Editor: Shao-Jun Tang, University of Texas Medical Branch, United States of America

Received September 19, 2013; **Accepted** December 16, 2013; **Published** January 22, 2014

Funding: This work was supported in part by Grant-in-Aid for Scientific Research (#23310137), and Global COE Program "Center of education and research for the advanced genome-based medicine for personalized medicine and the control of worldwide infectious diseases", from The Ministry of Education, Culture, Sports, Science and Technology (MEXT) Japan (http://www.mext.go.jp/). The funders had no role in study design, data collection and analysis, decision to publish, or preparation of the manuscript.

Competing Interests: The authors have declared that no competing interests exist.

* E-mail: furukawa@ims.u-tokyo.ac.jp

Introduction

Colorectal cancer is one of the most common malignancies worldwide, and the third most common cancer-related death in Japan and in the United States of America. In the US, it is estimated that 142,820 of new cases will be diagnosed and that 50,830 patients will die of this disease in 2013 (SEER stat fact sheets, http://seer.cancer.gov/statfacts/html/colorect.html) [1]. Although tumors at early stages are cured by surgery, those with far advanced stages are not curable by operation alone. Molecular targeted drugs, such as bevacizumab, cetuximab, and panitumumab, have been approved for the combination therapies to advanced colorectal cancer, and have improved the efficacy of chemotherapies. Nevertheless, the five-year survival rate of metastatic cancer is still lower than 12% [1], suggesting that novel therapeutic strategies are needed.

Molecular studies have clarified that deregulation of the Wnt signaling pathway is involved in colorectal carcinogenesis. Wnt signal regulates differentiation, proliferation, compartmentation, and cell fate of epithelial cells in the intestinal mucosa. One of the key mediators of the pathway is β-catenin, which also plays a structural role in cell-cell adhesion by binding to cadherins [2]. In the absence of Wnt signaling, a multi-molecular complex comprising of β-catenin, APC, Axin/Axin2 (or Conductin) and glycogen synthase kinase 3β (GSK3β) phosphorylates β-catenin, leading to its ubiquitination and subsequent degradation in the proteosome [3]. Upon binding with the Frizzled family and LRP receptor complexes, Wnt proteins activate Dishevelled (Dvl) proteins that inhibit activity of glycogen synthase kinase 3β [4]. As a result, degradation of β-catenin is suppressed and accumulated β-catenin induces TCF/LEF-mediated transcription [5,6].

In colorectal cancer cells, frequent mutations are observed in *APC*, the responsible gene for familial adenomatous polyposis of the colon, and *β-catenin (CTNNB1)* [4,7]. In hepatocellular carcinomas, frequent mutations are found in *CTNNB1* and *AXIN1* [4,8,9]. These mutations are mutually exclusive, and result in transactivation of TCF/LEFs, members of high mobility group (HMG) box protein family [5,9], suggesting that mutation in one of these components is enough to abrogate canonical Wnt signaling, and that TCF/LEF mediated transcriptional activation is important for these tumors. It has been thought that TCF4/β-catenin complex bend the DNA to access distant DNA region and form correct chromatin conformations for efficient RNA polymerase II (pol II)-mediated transcription [10]. Consequently, downstream target genes such as *c-myc* [11], *cyclinD1* [12], *MMP-7 (matrilysin)* [13,14], *urokinase-type plasminogen activator receptor (uPAR)* [15], *connexin 43* [16], *CD44* [17], *PPAR-delta* [18], *AF17* [19], *ENC1* [20], *Laminin-5 γ2* [21], *Claudin-1* [22] and *MT1-MMP* [23] are activated.

Earlier assigned as a hypothetical protein FLJ20315, RNF43 was shown to be an ubiquitin E3 ligase that associates with a nuclear protein, HAP95 [24]. Recently, two groups revealed that RNF43 enhances degradation of Wnt receptors including frizzled. One group showed that the degradation is mediated by the interaction with R-spondin proteins [25], and the other reported that this is carried out by endocytosis in LGR5-positive stem cells

in the intestine [26]. Interestingly, *RNF43* mutations were identified in a subset of pancreatic cancer [27,28], cholangiocarcinoma [29], colorectal cancer [30], and mucinous ovarian cancer [31]. These findings suggested that RNF43 is an important regulator of Wnt/β-catenin as well as Wnt/PCP pathway. In our earlier study, we found that expression of *RNF43* was frequently enhanced in colorectal cancer as well as hepatocellular carcinomas [32,33]. In addition, other groups revealed that *RNF43* expression was also elevated in adenomas of the colon [34], that it is down-regulated by a dominant-negative form of Tcf4 in LS174 colon cancer cells [35], and that expression of *RNF43* was induced by Wnt3a conditioned media [25]. These data suggested that *RNF43* is a downstream gene regulated by the Wnt-signaling pathway, but none has clarified the regulatory regions of its expression. In this study, we identified two Wnt-responsive elements (WREs) in intron2 of *RNF43* and found that these WREs are crucial for its transcriptional regulation through interaction with Tcf4/β-catenin complex. This is the first report of *RNF43* as a direct target of Tcf4/β-catenin complex and our data may be useful to understand the precise mechanism of RNF43 regulation.

Materials and Methods

Cell Lines

Human colorectal cancer cell lines, HCT116 and SW480, were obtained from the American Type Culture Collection (Manassas, VA). HCT116 cells were cultured in McCoy's 5A medium containing 10% fetal bovine serum (FBS, Life Technologies, Carlsbad, CA) and antibiotic/antimycotic solution (Sigma, St. Louis, MO). SW480 cells were cultured in Leibovitz's L-15 medium containing 10% FBS and antibiotic/antimycotic solution.

Gene Silencing

Human *CTNNB1*-specific siRNA were purchased from Dharmacon (ON-TARGETplus SMARTpool siRNA, L-003482-00). ON-TARGETplus Non-targeting Pool (D-001810-10) was used as a control. HCT116 or SW480 were seeded a day before treatment of siRNA. Cells were transfected with 15 nM of *CTNNB1*-specific or control siRNA using Lipofectamine RNAiMAX (Life Technologies). After 48 hours incubation, total RNAs were isolated with miRNeasy Mini Kit (Qiagen, Valencia, CA) according to the manufacture's instruction. The silencing effect was evaluated by quantitative RT-PCR and western blotting. Complementally DNA was synthesized from 1 μg of total RNA with Transcriptor First Strand cDNA Synthesis Kit (Roche Diagnostics GmbH, Mannheim Germany). Real-time PCR was performed using SYBR Green technology with sets of primers (*RNF43*: forward primer, 5′-GTTTGCTGGTGTTGCTGAAA-3′, reverse primer, 5′-TGGCATTGCACAGGTACAG-3′, *GAPDH*: forward primer, 5′-AGCCACATCGCTCAGACA-3′, reverse primer, 5′-GCCCAATACGACCAAATCC-3′) for *RNF43* on StepOnePlus (Life Technologies). Amounts of transcripts were determined by relative standard curve method, and *GAPDH* was used as internal control.

Preparation of Reporter Plasmids

Putative promoter regions in the 5′-flanking region of RNF43 were amplified by PCR with two sets of primers (forward primer, 5′-AAAACGCGTCTACAGGGGAAACAATGTTGAAGGT-CAATAGGCT-3′, and reverse primer, 5′-AAACTC-GAGTGGCCAGGTTTCTAGGCCCACTGC-3′ or 5′-AAACTCGAGTGGCAAAGAGAATGC-CAACTGGTGCTGT-3′, containing a recognition site of *Mlu*I or *Xho*I restriction enzyme (underlined nucleotides). PCR products were digested with the restriction enzymes and cloned into the appropriate enzyme sites of pGL3-Basic vector (Promega, Madison, WI). In addition, putative intronic enhancer region was amplified by PCR with sets of primers (fragment 1+2; 5′-AAAACGCGTAGACTATTTGGCTGTCTCAAAGT-CATTGCC-3′ and 5′-AAACTCGAGCCAGGGCCCAG-CATTGTGCCT-3′, fragment 1; 5′-AAAACGCGTAGAC-TATTTGGCTGTCTCAAAGTCATTGCC-3′ and 5′-AAACTCGAGTGGGGCATAGGCCCTGGTG-3′, fragment 2; 5′-AAAACGCGTCACCAGGGCCTATGCCCCAC-3′ and 5′-AAACTCGAGCCAGGGCCCAGCATTGTGCCT-3′, containing a recognition site of *Mlu*I or *Xho*I restriction enzyme (underlined nucleotides). PCR products were digested with the restriction enzymes, and cloned into the appropriate enzyme sites of pGL3-Promoter vector (Promega). Site-directed mutagenesis was carried out for both putative TCF4 binding sites, replacing CTTTGWW by CTTTGGC with the QuickChange II XL Site-Directed Mutagenesis Kit (Agilent Technologies, Santa Clara, CA) according to the manufacture's instruction.

Luciferase Assay

HCT116 or SW480 cells seeded on six-well plates were transfected with 1 μg of reporter plasmid and 0.1 μg of pRL-TK plasmid (Promega) by FuGENE 6 reagent (Roche) and incubated for 12 hours. Then the cells were further transfected with *CTNNB1* siRNA or control siRNA (ON-TARGETplus Non-targeting Pool #D-001810-10) at the concentration of 15 nM and incubated for an additional 36 hours. The cells were harvested and luciferase activities were measured using dual luciferase assay system (TOYO B-Net, Tokyo, Japan).

Chromatin Immunoprecipitation (ChIP) Assay

A ChIP assay was performed according to the Agilent Mammalian ChIP protocol with slight modifications. HCT116 or SW480 cells were cross-linked with 1% formaldehyde for 10 minutes at room temperature and quenched with 0.4 M glycine. Chromatin extracts were sheared by Micrococcal nuclease digestion, and subsequently protein-DNA complexes were immunoprecipitated with 3 μg of anti-TCF4 monoclonal antibody (6H5-3, Upstate, Charlottesville, VA) or anti-β-catenin monoclonal antibody (14/β-catenin, BD Transduction Laboratories, Franklin Lakes, NJ) bound to anti-mouse IgG-coated Dynabeads (Life Technologies). Non-immune mouse IgG (Santa Cruz Biotechnology, Santa Cruz, CA) was used as a negative control. The precipitated protein-DNA complexes were purified with the conventional DNA extraction method, and the DNAs were subjected to quantitative PCR analysis with the following primer sets; RNF43-int2-5′, forward primer, 5′-TCAACTCTCTGGA-TAAGGTGGAATAGC-3′, and reverse primer, 5′-GACTTTTGGGGTGGGTGGGAAATA-3′; RNF43-int2-3′, forward primer, 5′- TCGGGCACCTGGCCAAGATACA-3′, and reverse primer, 5′- TGGACGCCCTGGCTTCTGAG-3′. Specificity of the assay was determined by the amplification of a 5′-flanking region located from −4861 to −4768 of *RNF43* transcriptional start site using the following primers; forward primer, (−4861) 5′- CAAGGCTAGTCTGCCTCCAG-3′, reverse primer, (−4768) 5′- AGCGCTTTCCAAAGGAGGAA-3′. In addition, the amplifications of c-Myc (*MYC*) enhancer was used as a positive control (forward primer, 5′-GCTCAGTCTTTGCCCCTTTGTGG-3′, reverse, 5′- AA-CACCTTCCCGATTCCCAAGTG-3′).

Results

Knockdown of β-catenin Suppresses *RNF43*

To confirm that *RNF43* is regulated by the Wnt/β-catenin pathway, we measured expression levels of *RNF43* with or without β-catenin siRNA in HCT116 and SW480 cells (Figure 1A). HCT116 and SW480 cells exhibited constitutive activation of Wnt/β-catenin pathway through a mutation in *CTNNB1* or *APC*, respectively. Expectedly, quantitative RT-PCR disclosed that *RNF43* transcripts were markedly decreased by the depletion of β-catenin in these cells (Figure 1B). Consistently the protein level of RNF43 was reduced in SW480 cells treated with siCTNNB1 (Figure 1A). RNF43 protein was not detected in HCT116 cells because they harbor a homozygous mutation of *RNF43*. Since *RNF43* transcripts were more markedly decreased by siCTNNB1 in HCT116 than SW480, we used HCT116 cells for the analysis of regulatory region(s).

Promoter Analysis of *RNF43*

To identify the regulatory element(s) of Wnt-signaling in *RNF43*, we constructed three forms of reporter plasmids (RNF43-5′-1, RNF43-5′-2 and RNF43-5′-3) containing the 5′-flanking region and intronic regions of *RNF43*. RNF43-5′-1 contained approximately 1.6 kb (chr17:56494505–56496131, GRCh37), RNF43-5′-2 approximately 2.5 kb (chr17:56493599–56496131, GRCh37) and RNF43-5′-3 approximately 5.1 kb (chr17:56491044–56496131, GRCh37) of *RNF43*, respectively (Fig. 2A). These regions contained two elements, 5′-CTTTGAG-3′and 5′-CTTTGTC-3′, similar to the putative TCF/LEF-binding motifs (CTTTGWW) between −274 and −268, and between −54 and −48 of TSS, respectively. The reporter plasmids were transiently transfected with or without β-catenin siRNA in HCT116 cells, and luciferase activities were measured. As a result, we found that the luciferase activity of the cells transfected with RNF43-5′-1 or RNF43-5′-2 was significantly higher (approximately 3.0 and 2.5-fold, respectively) than that with empty vector, and that the activity of RNF43-5′-3 was similar to the empty vector (Fig. 2B). However, the knockdown of β-catenin did not affect the reporter activity of RNF43-5′-1 or RNF43-5′-2 (Fig. 2C). These data suggest that the 5.1-kb region contains the promoter but it does not include regulatory element(s) associated with Wnt/β-catenin signaling.

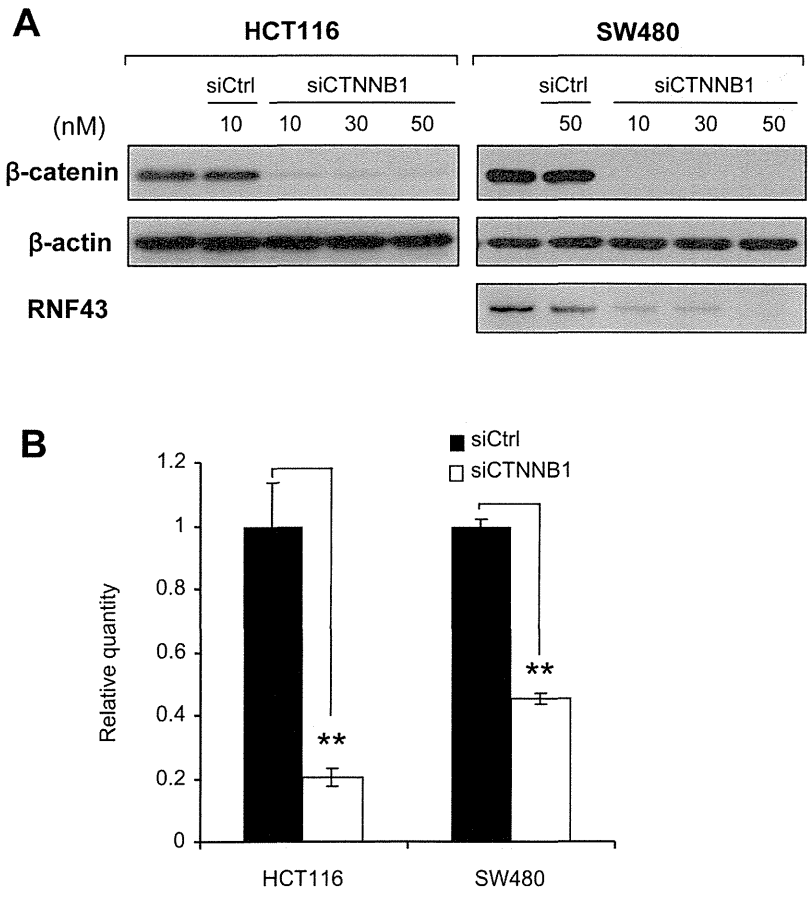

Figure 1. Effect of β-catenin depletion on *RNF43* expression. A) Knock down of β-catenin using *CTNNB1*-specific siRNA (siCTNNB1). HCT116 and SW480 cells were treated with siCTNNB1 or siCtrl, at the concentrations indicated in the figure. Expression levels of β-catenin and RNF43 were detected by western blotting with β-catenin- and RNF43-specific antibodies, respectively. B) Quantitative RT-PCR was carried out in triplicate using RNA from the cells. Cells were treated with 15 nM of *CTNNB1* siRNA (siCTNNB1) or control siRNA (siCtrl) for 48 hours. Relative expression of *RNF43* to the control siRNA is shown (mean ± standard deviation). A significant difference was determined by Student's t-test. **; $P<0.01$.
doi:10.1371/journal.pone.0086582.g001

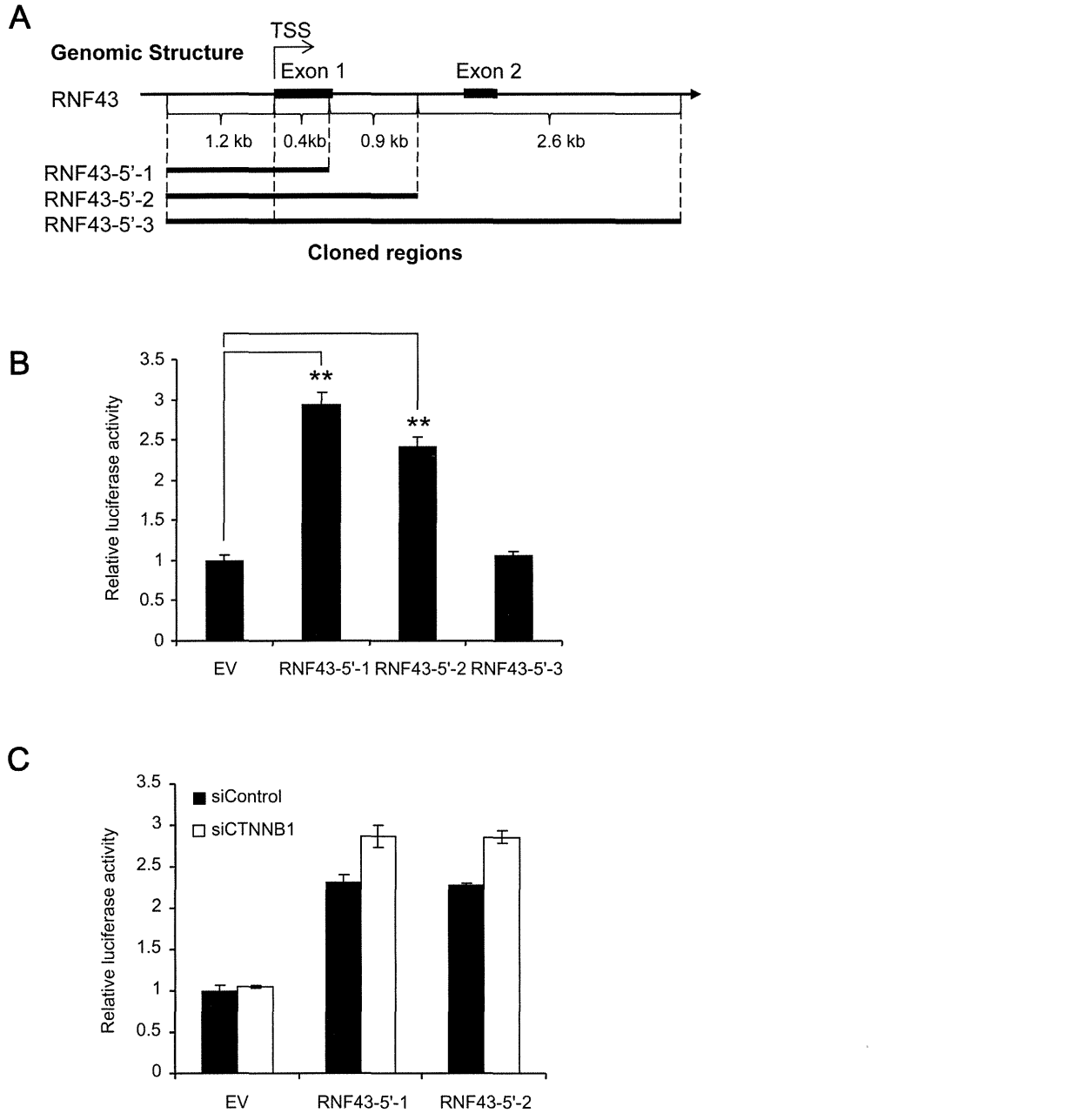

Figure 2. Promoter activity of the TSS-flanking region of *RNF43*. A) A genomic map of the TSS-flanking region of RNF43, and schematic representation of inserted regions in the reporter plasmids (pGL3-basic). TSS: transcription start site. B) Promoter activities of the reporter plasmids (mean ± standard deviation, **; $P<0.01$, Student's t-test). C) Effect of β-catenin depletion on the promoter activities (RNF43-5′-1 and RNF43-5′-2). EV: empty vector.
doi:10.1371/journal.pone.0086582.g002

Identification of WREs in *RNF43* Intron2

We next searched for putative regulatory regions in *RNF43* in public databases. A search in the ChIP-seq data of the ENCODE project (http://www.genome.ucsc.edu; The University of California Santa Cruz Genome Browser Database), identified four TCF4-enriched regions in the *RNF43* gene; one between −517 and +100 of TSS, two in intron2, and one in intron3. The two regions in intron2, but not the one in intron3, overlapped with RNA pol II-enriched regions. It is of note that these three regions were enriched with histone H3K4 mono-methylation. On the other hand, the region between −517 and −100 of TSS was enriched with pol II, histone H3K4 tri-methylation, and histone H3K27 acetylation, but not with histone H3K4 mono-methylation. Therefore we focused on the two regions in intron2 and tested whether they encompass TCF4-mediated transcriptional enhancer(s).

We then carried out a reporter assay using plasmids (RNF43-int2) containing a genomic region of 4.2 kb (chr17:56468435–56472609, GRCh37) encompassing the two TCF4-enriched regions in intron2. As we expected, the plasmids showed approximately 5-fold higher activity than empty promoter vector in HCT116 cells (Figure 3B). Importantly, the activity was significantly decreased by the treatment with β-catenin siRNA (Figure 3C). The β-catenin-dependent activation was also observed in SW480 cells (data not shown). These data strongly suggested that the 4.2 kb region might be involved in the Wnt-dependent transcriptional activation.

An additional search of transcription factor binding sites identified two putative TCF/LEF-binding motifs (CTTTGWW) in the regions; 5′-CTTTGAA-3′ and 5′-CTTTGAT-3′, which were termed putative Wnt-responsive element 1 and 2 (WRE1 and WRE2), respectively (Figure 3A). To clarify which element is crucial for the transactivation of *RNF43*, we prepared two forms of reporter plasmids containing either WRE1 or WRE2 (RNF43-int2-A and RNF43-int2-B, respectively). Although the luciferase

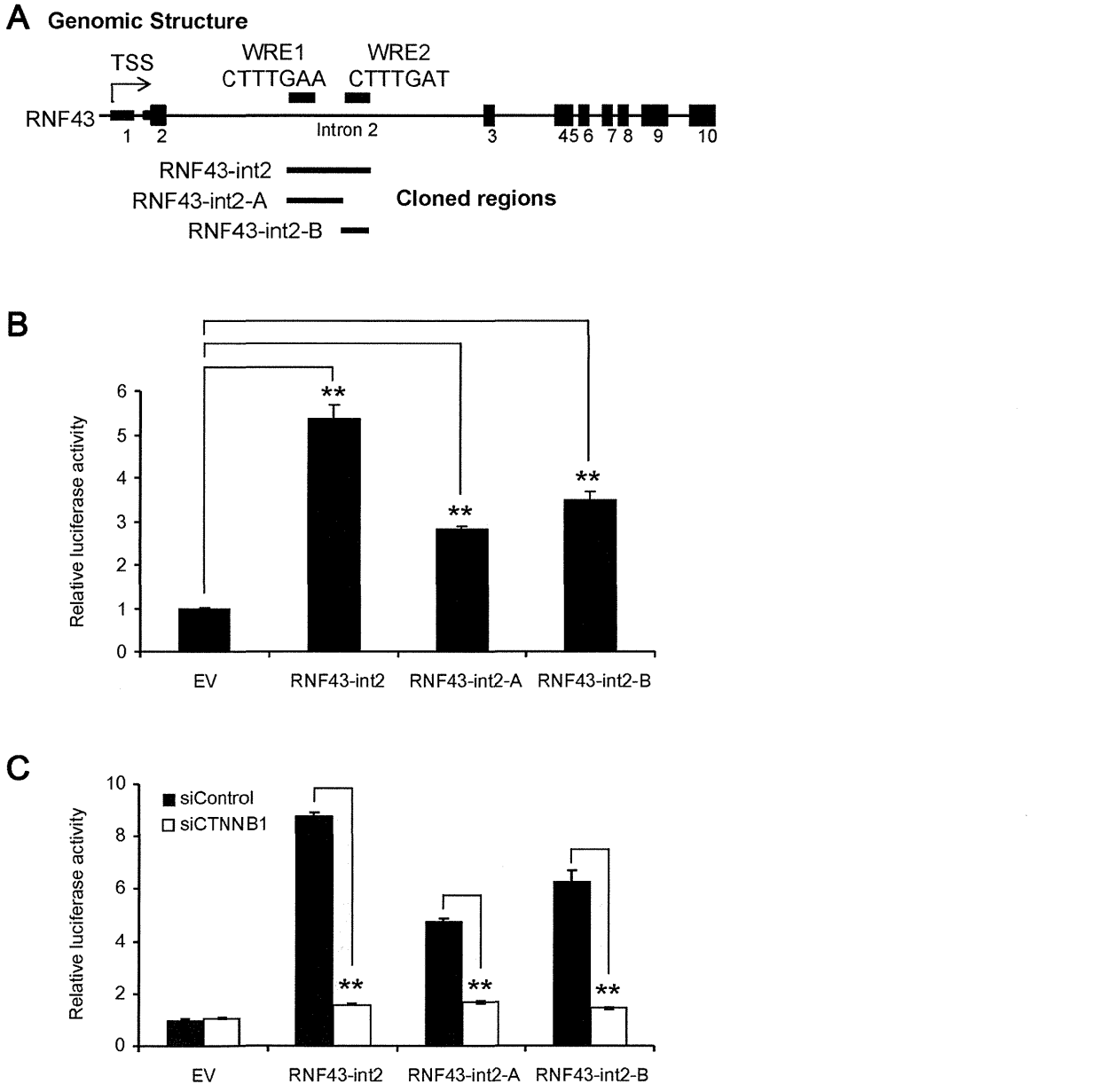

Figure 3. Luciferase assays with different regions in intron2. A) Schematic representation of Tcf4-enriched regions in the ENCODE data, and inserted regions in the promoter vector (pGL3-promoter). WRE: Wnt-responsive element. B) Enhancer activities were measured in triplicate using plasmids (RNF43-int2, RNF43-int2-A, and RNF43-int2-B) containing different regions in intron2 in HCT116 cells (mean ± standard deviation, **; $P<0.01$, Dunnett's test). C) Effect of β-catenin depletion on the enhancer activities (**; $P<0.01$, Student's t-test).
doi:10.1371/journal.pone.0086582.g003

activities of RNF43-int2-A and RNF43-int2-B were decreased at 57% and 65% of RNF43-int2, respectively, their activities were significantly higher than the control plasmids. In addition, co-transfection of β-catenin siRNA significantly suppressed both reporter activities (Figure 3C). We further generated mutant reporter plasmids containing substitution(s) in WRE1 and/or WRE2, from CTTTGWW to CTTTGGC (Figure 4A). Compared to the activity of wild type plasmids (RNF43-int2), reporter plasmids containing either substitution in WRE1 or WRE2 reduced the luciferase activity in HCT116 cells by 34% and 14%, respectively (Figure 4B). Similarly suppressed reporter activities were detected in SW480 cells (Figure 4C). Since combined substitutions in the WRE1 and WRE2 reduced the reporter activity by 36% in HCT116 cells and 71% in SW480 cells, other factor(s) may be involved in the enhanced reporter activity in HCT116 cells. Nevertheless, these data at least suggest that both elements should play a vital role in the β-catenin/TCF-dependent *RNF43* transactivation.

Interaction of WRE1 and WRE2 with TCF4/β-catenin Complex

To confirm whether TCF4 and β-catenin associates with WRE1 and WRE2, we conducted ChIP assays with TCF4-specific or β-catenin-specific antibody in HCT116 cells. Immunoprecipitation and subsequent quantitative PCR analysis revealed that the regions containing WRE1 and WRE2 were enriched by 7.3-fold and 28.1-fold with TCF4-specific antibody, respectively (Figure 5A). Of note, a WRE in the promoter of c-Myc, a direct target of β-catenin/TCF4 complex, was augmented about 13.6-fold in our analysis. Consistently, concordant enrichment of WRE1 and WRE2 was observed with β-catenin-specific antibody (Figure 5B). Similar results were obtained in SW480 cells, although the degree of enrichment was smaller than HCT116 (Figure 5C and 5D). These data indicated that the β-catenin/TCF4 complex interacts with WRE1 and WRE2 in intron2 of *RNF43*.

Discussion

In this study, we have identified regulatory regions of RNF43 transcription and showed that *RNF43* is a direct target gene of Tcf4/β-catenin complex. Our initial challenge to identify regulatory region(s) using reporter assay containing the 5′ flanking region successfully showed that the region is involved in its transcriptional activation, but failed to find region(s) associated with Wnt/β-catenin signaling. Subsequent search of the ENCODE database helped us to explore candidate regions that may interact with Tcf4. Regarding the decrease of reporter activity with RNF43-5′-3 plasmids containing the 5′ flanking region, intron 1, and a part of intron 2, the 3′ region of intron 1 and/or the 5′ region of intron 2 may have a repressive element(s) for the transcription.

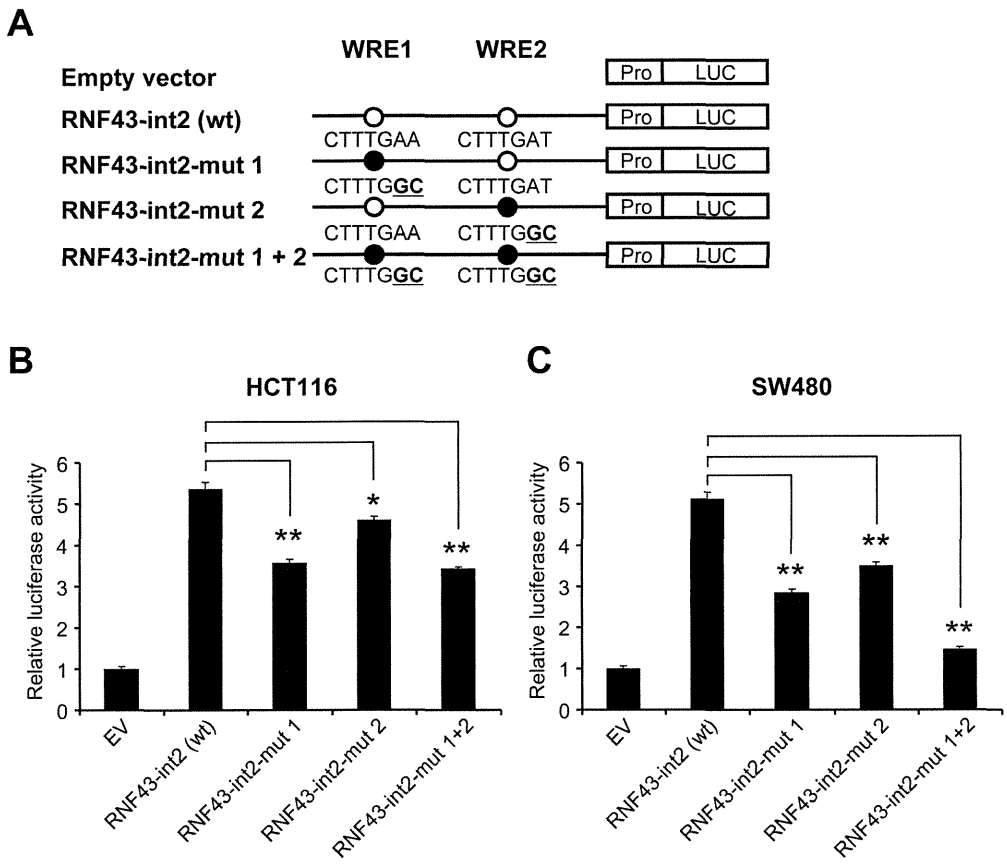

Figure 4. Involvement of WREs in the enhancer activity. A) Schematic representation of reporter plasmids containing substitution(s) in WRE1 and/or WRE2 (RNF43-int2-mut1, RNF43-int2-mut2, and RNF43-int2-mut1+2). B, C) Wild type or mutant reporter plasmids were transfected in HCT116 (B) and SW480 (C) cells, and luciferase activities were measured in triplicate (mean ± standard deviation, *; $P<0.05$, **; $P<0.01$, Dunnett's test).
doi:10.1371/journal.pone.0086582.g004

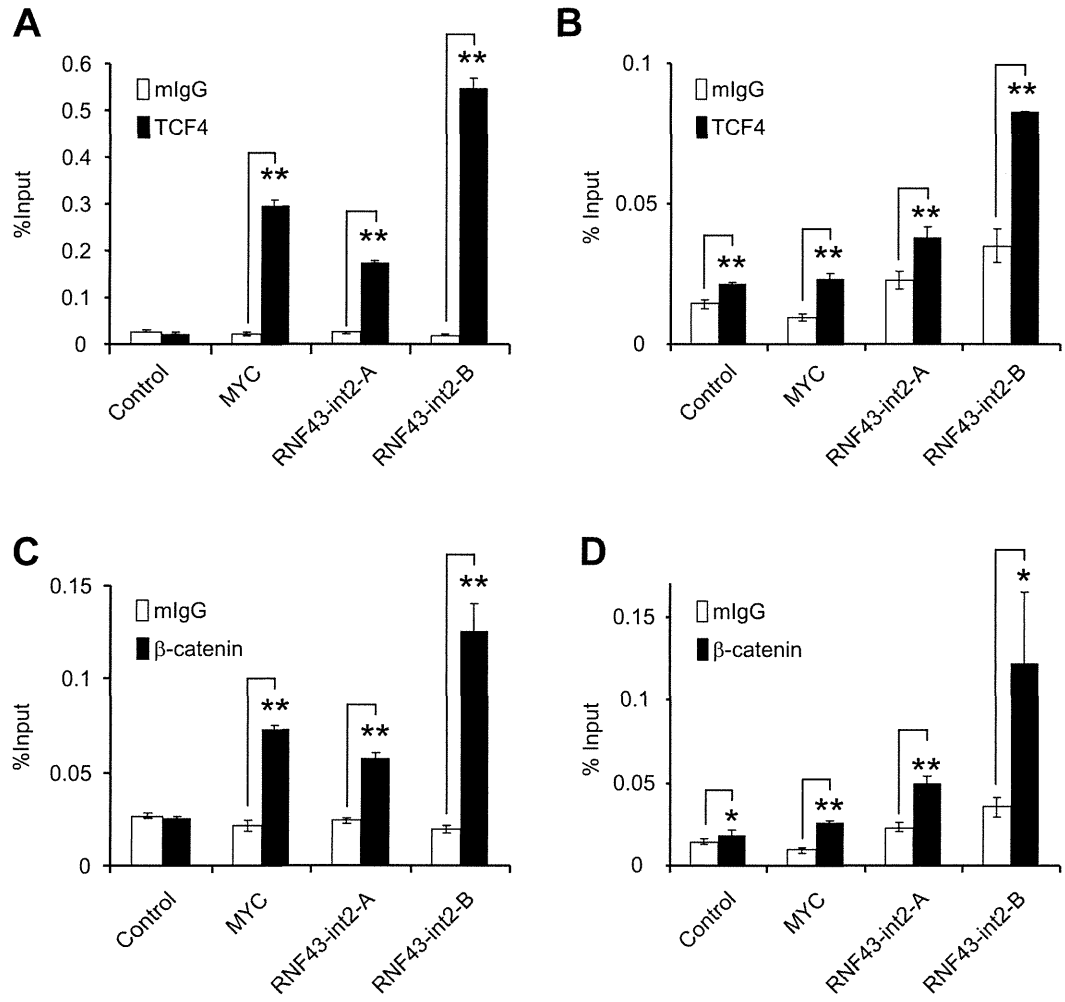

Figure 5. Association of the two WREs with Tcf4 and β-catenin. A, B) Quantification of precipitated regions by a ChIP assay with anti-TCF antibody was performed in HCT116 (A) and SW480 (B) cells using real-time PCR (mean ± standard deviation). Closed boxes indicate ChIP assay with anti-TCF4 antibody, and open boxes with control IgG. C, D) Quantification of precipitated regions by a ChIP assay with anti-β-catenin antibody in HCT116 (C) and SW480 (D) cells. A significant difference was determined by Student's t-test (*; $P<0.05$, **; $P<0.01$).
doi:10.1371/journal.pone.0086582.g005

Genome-wide approaches including ChIP-on-Chip and ChIP-seq analyses have helped to illustrate a global association map of transcription factors, chromatin occupancy, and histone modifications. As for the Tcf4-interacting regions, Hatzis *et al.* found a total of 6,868 enriched regions using tiling array [36]. By means of luciferase-reporter assays, they examined 22 regions of approximately 1000 bp containing at least one of the enriched regions. Consequently, 10 of the 22 increased the activity, and 9 of them were down-regulated by the cotransfection with dominant negative Tcf4, suggesting that the enriched regions do not always play a role in transcriptional activation or associate with Tcf4/β-catenin. Their data included a Tcf4-enriched peak in intron2 of *RNF43* (chr17:53823246, NCBI35/hg17), this peak was close to WRE2 (chr17:53824064–53824070, NCBI35/hg17) suggesting a consistency of transcription factor-binding regions detected by ChIP-on chip in spite of different cell lines they used. They also reported that the Tcf4-binding sites are distributed along the genome, and 18% of them were located in intragenic regions further than 10 kb from the TSS. Consistently, the two WREs of *RNF43* were located at approximately 22 kb downstream of TSS. In addition, their data unveiled that 31% of peaks were located in the 5′-flanking region at a great distance from TSSs. In the case of c-Myc, WREs localized to a region over 400 kb upstream from the gene are involved in chromatin looping in response to the activation with serum mitogens [37]. Therefore additional WREs may play a role for the transcriptional regulation of RNF43 in combination with WRE1 and WRE2.

In addition to Tcf4, genome-wide approaches including serial analysis of chromatin occupancy (SACO) and ChIP-seq have been applied to identify the regions interacting with β-catenin [38,39]. In agreement with our findings, the list of 412 β-catenin-interacting regions detected by SACO included a region containing the Tcf consensus motif in RNF43 (Chr17:53824041 NCBI35/hg17), which corresponded to WRE2 in our data. The same group later carried out a ChIP-seq analysis and identified a total of 2,168 enriched regions with β-catenin in HCT116 cells. In the list of the 2168 regions, three were located in intron2 of RNF43 (chr17:53819951–53820630, chr17:53823671–53824270,

and chr17:53826701–53827401, NCBI36/hg18) [39]. Notably, WRE1 and WRE2 are within two of three enriched regions, suggesting that ChIP-seq is a powerful tool to discover binding regions of transcription factors.

In this study, we incorporated the data of histone modifications and occupancy of RNA pol-II. Consistent with the view that histone H3K4 mono-methylation and an interaction with RNA polymerase II are the hallmarks of transcriptional enhancers, the two WREs in intron2 played a vital role as a transcriptional enhancer in our luciferase assay. Meanwhile, the 5′-flanking region of 2.4 kb was associated with RNA polymerase II and histone H3K4 tri-methylation suggesting that this region served for the constitutive transcriptional activation through the remodeling of heterochromatin complex to euchromatin state. Although the ENCODE data depicted a peak of Tcf4-binding in the 5′-flanking region, enrichment of multiple transcription factors was observed in the same region. Therefore the peak of Tcf4 may be a false positive. Alternatively Tcf4 may interact with that region without the recruitment of β-catenin. Since the data of histone modifications and RNA pol-II occupancy are useful information to predict the chromatin structure of interacting regions and their transcriptional activity, future studies on a global association map of β-catenin and Tcf4 with histone modifications will gain an insight into the dynamic transcriptional regulation played by Tcf4/β-catenin and chromatin modification enzymes such as Brg1, TRRAP, TIP60, CBP/p300, and MLL [10].

Recently, it was reported that RNF43 and ZNRF3, transmembrane E3 ubiquitin ligases, selectively ubiquitinate frizzled receptors and targets them for degradation. RNF43 and ZNRF3, a homologue of RNF43, are highly conserved in vertebrates, and associate in the membrane with frizzled receptors and low density lipoprotein receptor-related proteins, LRP5/6. RNF43 promotes endocytosis of frizzled receptors including FZD1 and FZD3, and suppresses Wnt/β-catenin responses [26]. ZNRF3 also promotes the turnover of frizzled receptors and LRP6. Interestingly inhibition of ZNRF3 enhances Wnt/β-catenin signaling and suppresses Wnt/planar cell polarity signaling [25]. These data suggested that ZNRF3 and RNF43 regulate canonical and non-canonical Wnt pathway. Our data, in line with others, suggest that RNF43 functions as a negative feedback regulator modulated by Tcf4/β-catenin complex. This notion is reminiscent of *AXIN2*, and *DKK1*, which are also downstream targets of the canonical Wnt signaling pathway and negatively regulate the signals in different manners [40,41,42,43,44]. Regarding the tumorigenesis of pancreatic and ovarian cancers, inactivating mutations in *RNF43* are supposed to abrogate Wnt signaling including canonical and non-canonical pathways. However, the effect of negative feedback by the enhanced expression of RNF43 has not been clarified in colorectal or liver cancer. Although the augmented transcriptional activity of Tcf4/β-catenin complex by inactivation mutations in *APC* or *AXIN2*, or activating mutations in *CTNNB1* may not be affected by the suppression of frizzled receptors, complex network of signaling pathways may render undetermined characteristics to colorectal and liver cancer cells, as restoring expression of *SFRP4* and *DKK1* in colorectal cancer cells attenuates Wnt signaling [44,45]. Further investigations on the effect of enhanced or suppressed RNF43 function may shed light on the undetermined networks associated with canonical and non-canonical Wnt pathways, and may contribute to the development of diagnostic, therapeutic, and/or preventive strategies to human diseases.

Acknowledgments

We thank Seira Hatakeyama (The University of Tokyo) for her technical assistance.

Author Contributions

Conceived and designed the experiments: NT YF. Performed the experiments: NT KY. Analyzed the data: NT KY. Contributed reagents/materials/analysis tools: TI TF KY. Wrote the paper: NT YF.

References

1. Siegel R, Naishadham D, Jemal A (2013) Cancer statistics, 2013. CA Cancer J Clin 63: 11–30.
2. Nelson WJ, Nusse R (2004) Convergence of Wnt, beta-catenin, and cadherin pathways. Science 303: 1483–1487.
3. Rubinfeld B, Albert I, Porfiri E, Fiol C, Munemitsu S, et al. (1996) Binding of GSK3beta to the APC-beta-catenin complex and regulation of complex assembly. Science 272: 1023–1026.
4. Polakis P (2000) Wnt signaling and cancer. Genes Dev 14: 1837–1851.
5. Behrens J, von Kries JP, Kuhl M, Bruhn L, Wedlich D, et al. (1996) Functional interaction of beta-catenin with the transcription factor LEF-1. Nature 382: 638–642.
6. Molenaar M, van de Wetering M, Oosterwegel M, Peterson-Maduro J, Godsave S, et al. (1996) XTcf-3 transcription factor mediates beta-catenin-induced axis formation in Xenopus embryos. Cell 86: 391–399.
7. Kinzler KW, Vogelstein B (1996) Lessons from hereditary colorectal cancer. Cell 87: 159–170.
8. Guichard C, Amaddeo G, Imbeaud S, Ladeiro Y, Pelletier L, et al. (2012) Integrated analysis of somatic mutations and focal copy-number changes identifies key genes and pathways in hepatocellular carcinoma. Nat Genet 44: 694–698.
9. Laurent-Puig P, Legoix P, Bluteau O, Belghiti J, Franco D, et al. (2001) Genetic alterations associated with hepatocellular carcinomas define distinct pathways of hepatocarcinogenesis. Gastroenterology 120: 1763–1773.
10. Mosimann C, Hausmann G, Basler K (2009) Beta-catenin hits chromatin: regulation of Wnt target gene activation. Nature Reviews Molecular Cell Biology 10: 276–286.
11. He TC, Sparks AB, Rago C, Hermeking H, Zawel L, et al. (1998) Identification of c-MYC as a target of the APC pathway. Science 281: 1509–1512.
12. Tetsu O, McCormick F (1999) Beta-catenin regulates expression of cyclin D1 in colon carcinoma cells. Nature 398: 422–426.
13. Brabletz T, Jung A, Dag S, Hlubek F, Kirchner T (1999) beta-catenin regulates the expression of the matrix metalloproteinase-7 in human colorectal cancer. Am J Pathol 155: 1033–1038.
14. Crawford HC, Fingleton BM, Rudolph-Owen LA, Goss KJ, Rubinfeld B, et al. (1999) The metalloproteinase matrilysin is a target of beta-catenin transactivation in intestinal tumors. Oncogene 18: 2883–2891.
15. Mann B, Gelos M, Siedow A, Hanski ML, Gratchev A, et al. (1999) Target genes of beta-catenin-T cell-factor/lymphoid-enhancer-factor signaling in human colorectal carcinomas. Proc Natl Acad Sci U S A 96: 1603–1608.
16. van der Heyden MA, Rook MB, Hermans MM, Rijksen G, Boonstra J, et al. (1998) Identification of connexin43 as a functional target for Wnt signalling. J Cell Sci 111 (Pt 12): 1741–1749.
17. Wielenga VJ, Smits R, Korinek V, Smit L, Kielman M, et al. (1999) Expression of CD44 in Apc and Tcf mutant mice implies regulation by the WNT pathway. Am J Pathol 154: 515–523.
18. He TC, Chan TA, Vogelstein B, Kinzler KW (1999) PPARdelta is an APC-regulated target of nonsteroidal anti-inflammatory drugs. Cell 99: 335–345.
19. Lin YM, Ono K, Satoh S, Ishiguro H, Fujita M, et al. (2001) Identification of AF17 as a downstream gene of the beta-catenin/T-cell factor pathway and its involvement in colorectal carcinogenesis. Cancer Res 61: 6345–6349.
20. Fujita M, Furukawa Y, Tsunoda T, Tanaka T, Ogawa M, et al. (2001) Up-regulation of the ectodermal-neural cortex 1 (ENC1) gene, a downstream target of the beta-catenin/T-cell factor complex, in colorectal carcinomas. Cancer Res 61: 7722–7726.
21. Hlubek F, Jung A, Kotzor N, Kirchner T, Brabletz T (2001) Expression of the invasion factor laminin gamma2 in colorectal carcinomas is regulated by beta-catenin. Cancer Res 61: 8089–8093.
22. Miwa N, Furuse M, Tsukita S, Niikawa N, Nakamura Y, et al. (2001) Involvement of claudin-1 in the beta-catenin/Tcf signaling pathway and its frequent upregulation in human colorectal cancers. Oncol Res 12: 469–476.
23. Takahashi M, Tsunoda T, Seiki M, Nakamura Y, Furukawa Y (2002) Identification of membrane-type matrix metalloproteinase-1 as a target of the beta-catenin/Tcf4 complex in human colorectal cancers. Oncogene 21: 5861–5867.
24. Sugiura T, Yamaguchi A, Miyamoto K (2008) A cancer-associated RING finger protein, RNF43, is a ubiquitin ligase that interacts with a nuclear protein, HAP95. Exp Cell Res 314: 1519–1528.